EUROPEAN COMMISSION

Community research

Climate Information Portal

CLIPC DELIVERABLE (D -N°: 7.2)

The use of impact functions to develop Tier 2 and 3 indicators in CLIPC

Dissemination level: PU (public)

Lead Authors: ***Luís Costa, Mikael Hildén, Rob Swart, Linda Krummenauer, Milka Radojavic, Juha Pöyry***

Contributing authors: ***Juliane Otto, Kristin Bottcher, Stefan Fronzek,***

Reviewer(s): **Juliane Otto**
Peter Thijsse

Release date for review: 26-11-2015

Final date of issue: 14-12-2015

Revision table			
Version	**Date**	**Name**	**Comments**
1	23-11-2015	Mikael Hilden	Structure and language
2	25-11-2015	Rob Swart	Structure and language
3	8-12-2015	Juliane Otto	Consistency check and outcomes
4	11-12-2015	Peter Thijsse	External view to WP7

Abstract

This deliverable explores the possibility of deriving impact indicators based on empirical impact functions. A review on previous use of impact functions in the literature led to the elaboration of two approaches for establishing impact functions in CLIPC for the elaboration of impact indicators. To demonstrate the potential application, three new impact indicators for CLIPC are elaborated using the two approaches. These are: **Moth Phenology**, **Threshold Mortality Temperatures**, and **Potential Economic Damages from Coastal Flooding**. The advantages, uncertainties, saliency, legitimacy, and credibility are also described for each new indicator. Finally, the approach described in this report suggests that the development and use of impact functions is a feasible and attractive way for developing Tier 2 and 3 indicators that are salient for policy makers. An explorative approach should be encouraged by making relevant data available, but care needs to be taken to ensure the credibility of any resulting impact functions.

Project co-funded by the European Commission's Seventh Framework Programme (FP7; 2007-2013) under the grant agreement n°607418

Table of contents

List of figures:

Executive Summary

Objectives:

The objective of this deliverable is twofold. First, the deliverable reviews the methodological challenges of generating impact functions. An impact function is described as a quantitative relationship between a climate or climate related stimulus (e.g., temperature or flood depth), and an ecological or socio-economic variable (e.g., economic loss or species distribution). The review identifies two approaches for establishing impact functions that can be used in CLIPC for the development of additional impact indicators. The first approach is based on establishing a statistical relationship between a climate variable, or Tier 1 indicator, and a measure of socio-economical or ecological impact for a particular large region, e.g. Europe-wide. Because socio-economic and ecological data is not always available across Europe at a temporal or spatial resolution required for a statistical assessment, a second approach was established. The latter uses impact functions that have been derived from statistics for a particular location and scale these up, either using additional variables or generalized assumptions, so that the function can be used at much larger spatial scales than that for which it was originally developed. In order to demonstrate potential applications, three impact indicators for CLIPC are elaborated these are: **Moth Phenology Indicator**, **Threshold Mortality Temperatures**, and **Potential Economic Damages from Coastal Flooding**.

Although work on the new indicators is still preliminary, it serves to highlight the benefits, and also challenges, of using impact functions to generate impact indicators. Therefore, the benefits, uncertainties, saliency, legitimacy, and credibility of each additional indicator are also described. The potential inclusion of each indicator in the CLIPC portal is discussed.

Results:

The indicators developed using impact functions are: **Moth Phenology Indicator**, **Threshold Mortality Temperatures**, and **Potential Economic Damages from Coastal Flooding**. These new indicators illustrate the approach and have a number of useful characteristics for potential users of the CLIPC portal.

The **Moth Phenology Indicator** illustrates that it is possible to project the timing of peak flight periods of moths using temperature observations and satellite data. The use of remotely-sensed variables (snow melt, greening) in the impact function makes it possible to determine the phenology of species over large geographic areas. Potentially practical applications include the management of pest insect populations in a changing climate.

The **Threshold Mortality Temperatures** indicator allows better contextualizing of heat data than purely temperature based indicators such as number of hot days (TIER 1 indicator). This shows that the salience and relevance of the temperature information can be increased through impact functions. Thus, the actual impacts on the population of a change in, for example, the number of hot days, will depend on the minimum human mortality temperatures. The

indicator can therefore be interpreted as the current level of tolerance to heat by the population. Another asset of the indicator is that it provides a first order approximation of threshold temperatures in locations where so far no specific heat-mortality study has been conducted.

The **Potential Economic Damages from Coastal Flooding** indicator is determined via a systematic transformation of location-specific surge heights into an estimate of economic damages associated with different land-uses. The impact function estimates economic damages derived for specific areas can be generalised and compared with existing observations of economic losses from insurance or disaster data covering wider areas. In this manner, it opens the way for indicator validation. Using the empirical damage functions associated with different types of land-use and time horizons allows the support of discussions on urban adaptation to coastal flooding by highlighting different levels of adaptation, including actions that modify the function itself through preventive measures at the land-use scale that change the response between flood depth and economic damage.

Perspectives:

The approach described in this report suggests that the development and use of impact functions is a feasible and attractive way of increasing the relevance and salience of purely physical indicators of climate change (i.e. Tier 1 indicators). Impact functions can also be used to scale up detailed information from Tier 2 or Tier 3 indicators developed for specific locations to cover wider areas. Such indicators have been developed and published in the scientific literature by various authors, but the data are generally not publicly available and can therefore not easily be included in CLIPC.

Caution is warranted in interpreting indicators based on impact functions as there are significant uncertainties related to the data, the choice and estimation of the impact function and the attribution of impacts to climate change. But because of the attractiveness of enabling users to explore new impact indicators in a quick way on their own, it is recommended to further explore opportunities for combining Tier 1 indicators with other information to produce Tier 2 and 3 indicators based on impact functions. However, despite some promising work the challenges in using impact function for constructing higher Tier indicators should not be underestimated. This report provides ideas for how indicators can be generated using impact functions, but the specific methods will depend strongly on the nature of the impact to be evaluated and on the availability of data.

1. Introduction

The review of indicators conducted in deliverable 7.1 revealed that, in general, there are fewer Tier3 climate change indicators than Tier2 indicators and much fewer than Tier-1 indicators. A similar distribution of indicators classified into Tiers 1, 2 and 3 can be seen in studies such as EEA (2012) and ISI-MIP (see sections 2 and 5 of deliverable 7.1). An important reason for this is that while most Tier 1 and some Tier 2 indicators are based on direct observations, the derivation of Tier 3 indicators often requires extensive, model-based, exercises that combine information on bio-physical conditions with information on the society in order to credibly link observations to climate change impacts.

The composite nature of Tier 3 indicators (and those Tier 2 indicators that are based on similar combinations of different sources of information) increase the number of sources of uncertainty and make the use of these indicators more dependent on context than Tier 1 indicators. Efforts to develop Tier 3 indicators have been often restricted to the national or subnational scale, although larger-scale (e.g., Europe-wide) examples of Tier 2 and 3 indicators are becoming more frequent. For example the economic results of projects such as PESETA I and II[1] have aimed at pan-European indicators for the costs of climate change.

Many users of the CLIPC portal are likely to be particularly interested in Tier 2 and 3 indicators (see Deliverables 2.1 and 2.2). This includes users engaged in awareness raising, risk assessment and developing climate responses to reduce climate change impacts. This is in line with one of the priority purposes for the indicators and data provided by CLIPC which is to "*support the development of adaptation strategies and plans*", in particular for "*intermediate organizations*" and "*societal end-users*" (see CLIPC deliverable 2.1).

In this deliverable the possibilities to develop indicators based on inductive reasoning is explored. In practice, it implies using data for building statistical models that describe observed impacts using selected indicating variables tested for statistical significance (Hinkel 2011). Inductive reasoning is one of the ways that CLIPC aims at responding to the original call text which asked for functionalities to "build" new indicators. However, due to data constraints mainly in regard to damage, health and other socio-economic impacts, and the limited feasibility to simplify the system of analysis in a meaningful way, "additional" or "new" indicators, as mentioned in the call text, cannot yet compose a large fraction of the indicator sets to be provided in CLIPC. Feasibility and scientific credibility have to be taken into account and many new indicators are still in an early exploratory phase.

The concept of impact function (which can also be named damage function) is the core of the inductive approach followed in this deliverable. An empirical impact function characterises the relation between a given societal/bio-physical impact (e.g., human lives, species distribution, agricultural yield, economic damages) and explanatory variables (e.g., maximum flood-level, temperature). Generically speaking, an impact function establishes the shape of

[1] http://peseta.jrc.ec.europa.eu/economic_results.html

the relationship between a climate-related stimulus and a given (societal) impact in a quantitative fashion. The calculation of impact functions fills a gap between using complex impact modelling, (e.g., HAZUS-HM, see Vickery 2009) and a deductive approach that combines information on climate exposure with socio-economic sensitivity data.

Impact functions constitute an intermediate level of complexity for impact assessment. It should be stressed that deriving impact functions from a statistical analysis is accompanied by many uncertainties. A significant statistical relationship is not a conclusive proof of a causal relationship and cannot as such be used for attribution purposes. Usually, climatic variables or Tier 1 indicator(s) constitute only a part of a much larger set of factors driving particular observable changes. Nevertheless, the examples provided illustrate impact functions that are supported by more complex analyses that link the Tier 1 indicator to the Tier 3 impacts. Similarly, this deliverable also explores cases where Tier 1, combinations of Tier 1 indicators, or climatic variables, can be transformed into Tier 2 indicators.

The objective of this deliverable is two-fold:

- The first is to explore existing approaches from the literature that, despite data constraints, have established a relationship between climate stimuli (a terms used here as comprising climate variables, Tier 1 or 2 indicators or climate-related hazards e.g., flood frequency and height) and a (Tier 3) measure of impact on societies or ecosystems. Impact can in this case refer to a multitude of dimensions such as economic losses, human lives, infrastructural damages or species distributions. Such work has served to integrate climate change damage in Integrated Assessment Modelling (IAM), often at continental or global scale, including agriculture, health, sea-level rise (flooding), non-market damages and/or catastrophic damages (e.g., Ortiz and Markandya, 2009). From the examples collected and lessons learned, general approaches for the elaboration of impact functions in CLIPC are produced. This part of the objective is reported in sections 2 and 3.
- The second objective of this deliverable is to present ongoing work in CLIPC to explore additional indicators that take advantage of newly-produced or existing damage functions. The examples are described in regard to a) description of the approach and results; b) advantages, uncertainties, saliency, legitimacy and credibility; and c) potential use in the CLIPC portal. These examples cover the three overarching themes of CLIPC. This work is described in section 4.

2. Theory and approaches for specifying impact functions in CLIPC

a) Empirically-based impact functions

Empirical investigations of the relationship between climate and socio-economic impact have been mostly carried out at a regional or local scale, although relationships between climate and socio-economic impacts are also noted at global and continental scales. Examples of the latter include analyses of agricultural production changes (Lobell et al 2011) and human mortality due to heat (Ballester et al, 2011), respectively. Impact functions are in common use

in hazard analysis (Boettle et al 2011, Prahl et al, 2012, Merz et al, 2010), economic estimates of climate change impacts (Ciscar et al, 2011) or in the investigation of specific effects such as crop changes under climate change (Schlenker et al, 2009). Although in general data availability remains an issue, a growing number of examples are increasingly made available in literature, offering possibilities to learn from the experiences on how to establish impact functions. The shape of the climate-impact relationship is conditional on the nature and scale of the impact to be evaluated. Some of the most common shapes are highlighted by in Figure 1.

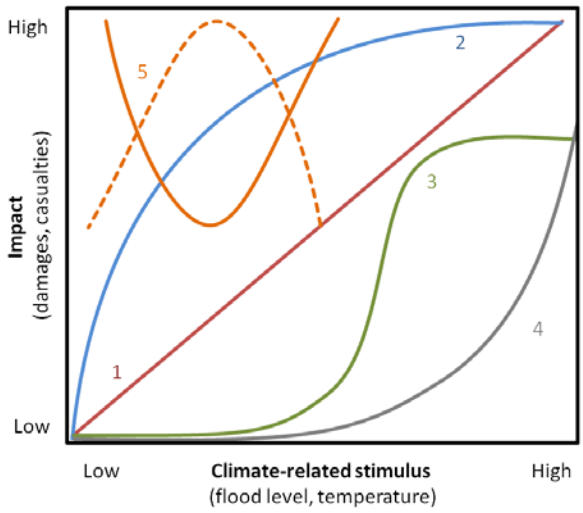

Figure 1 - Stylized relationship between climate-related stimulus and socio-economic impact, namely, linear (curve 1), concave (curve 2), s-shape (curve 3), convex (curve 4), u-shape and inverted u-shape (curves 5).

Linear

A linear relationship between climate stimulus and impact is one of the simplest assumed shapes. It is characterized by impacts growing in the exact same proportion for each increasing unit of climate stimuli. Such relationships have been investigated for the occurrence of extremes in precipitation and their impact on kharif foodgrain yield over India (Revadekar 2012) see Figure 2. In some cases a transformation of the original data can yield a linear relationship: for example the logarithm of monthly area burnt and monthly 90th percentile of daily maximum temperature in Portugal was found to be linearly correlated (Carvalho et al, 2008). Because of its simplicity, a linear relationship between climate stimuli and climate impact is likely to be valid only for a restricted range of the impact processes it tries to capture.

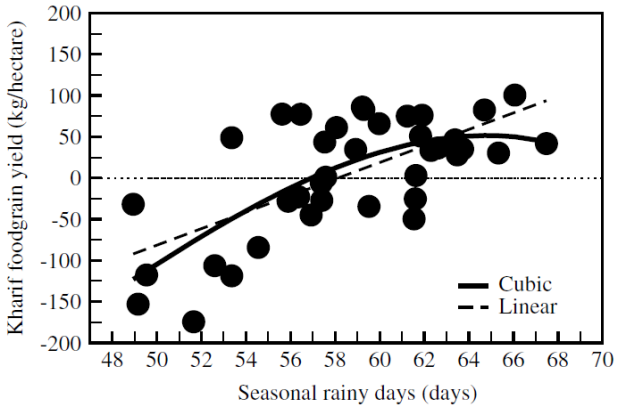

Figure 2 – Relation between Karif foodgrain yield and rainy days (Revadekar 2012).

Concave and convex

A concave relationship (see Hydrotec curve in Figure 3) between climate stimulus and impact has been used in describing *relative* damages associated with a given inundation height (defined here as the difference between the water level and the building foundation) at the level of an individual building. The shape considered accounts for a saturation of damages (impact) for very high magnitudes of climate stimulus. The exact curvature of impact function is influenced by the building characteristics such as type (residential, commercial), construction materials (concrete, wood) or floor space (Dutta et al, 2003). The impact has been expressed as fraction of value lost or percentage of damages to the structure, contents or both. Although the concave shape of the function for flooding has been observed across different geographical contexts, other shapes are possible, for example linear or convex (Boettle et al 2011, Merz et al 2010) and exemplified also in Figure 3.

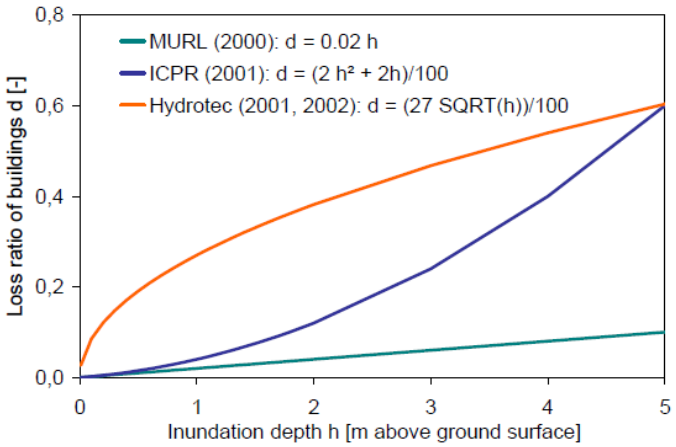

Figure 3 – Left: Examples of depth-damage-curves for the residential sector typically used in Germany[2] [3] [4] (Merz et al 2010)

Even though the damages of each single building can be described by a supra-linear shape, the resulting cumulative economic impacts assume an exponential shape.

[2] MURL - Ministerium fuerur Umwelt, Raumordnung und Land-wirtschaft des Landes Nordrhein-Westfalen

[3] ICPR - International Commission for the Protection of the Rhine

[4] Hydrotec - https://www.hydrotec.de/

S-shape

Impact functions taking the form of an s-shape have been used in work determining economic damages associated with wind hazard (Prahl et al. 2012) and loss of human life with increasing flood depths (Boyd et al. 2005).

For winter storms affecting Germany, Prahl et al. (2012) developed damage function based on the presumption of a power law-based sigmoid curve, see Figure 4. Economic damage data was represented by insurance-loss data from the years 1997 to 2007[5], comprising daily losses due to wind and hail for 439 German administrative districts. For representing the climate stimulus, data of daily maximum wind speed was used. The relation established reveals a strong increase for wind speeds higher than approximately 13 ms^{-1} and an approximately constant regime for lower wind speeds. In this particular case, the predictive power of wind speeds in representing insurance-loss data at the district level was assessed. When all German districts are considered, R^2 is between 0.2 and 0.6, with an average value across Germany of 0.4. The highest correlations were generally obtained for relatively flat regions with high frequency of strong winds. Insurance losses could be well described by power-law damage functions with regionally varying exponents using daily maximum wind speed as explanatory variable. The differences in R^2 across German districts allowed for the identification of broader regions for which the model developed performs relatively better than for other regions.

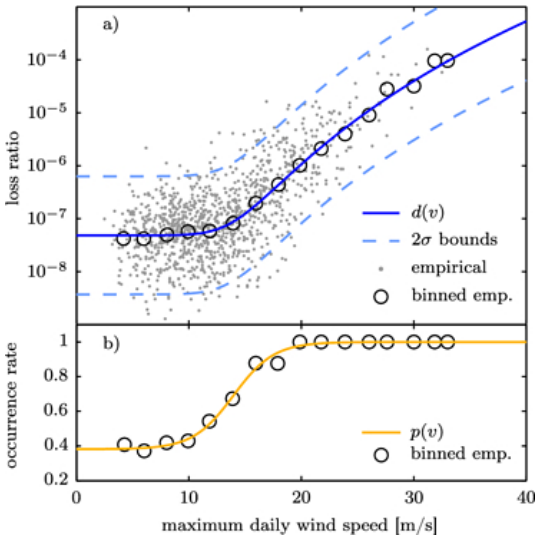

Figure 4 - Empirical loss data for an arbitrarily chosen German district from Prahl et al. (2012)

When trying to establish impact functions between flood events and loss of human life in floods, the issue of data scarcity becomes increasingly problematic. Boyd et al. (2005) derived a mortality function based on observations from only seven flood events, including hurricanes Betsy (1965) and Camille (1969) in the United States. The author proposed a relationship

[5] Provided by the German Insurance Association (Gesamtverband der Deutschen Versicherungswirtschaft e.V., GDV)

between mortality and water depth shown in Figure 5. The s-shaped function possesses an asymptote for mortality equal to 0.34 for water depth values of approximately above 4 meters.

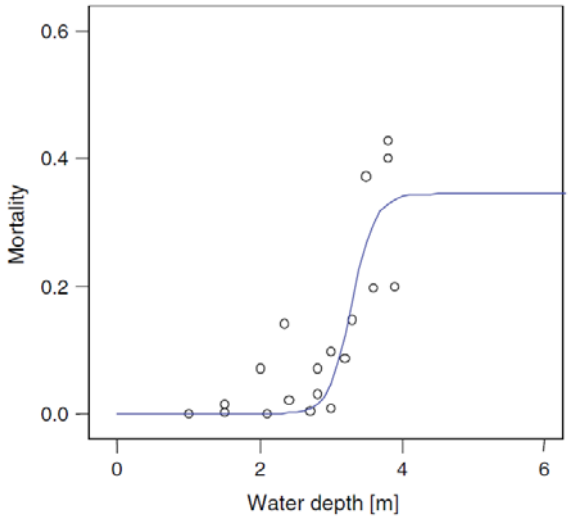

Figure 5 . Proposed relationship between mortality and water depth based on observations from historical hurricane flood events in Boyd et al, (2005) on the right

In a flood event, there is always a considerable fraction of survivors and hence it would be important to estimate the point at which the saturation starts. In this particular case, there is no evidence for saturation at water depths above 4m as there is no data for floods with water depth higher than 4m. Accordingly, the function rather arbitrarily implies that mortality is constant after 4 meters of inundation. This may lead to flawed estimates of the consequences of severe floods. For the Netherlands, Van den Hengel (2007) proposes to estimate mortality based not only on the water depth but also on the rate at which water raises during a flood event.

U-shape

For the case of health impacts attributable to heat events (e.g., mortality or morbidity) usually a U-shape relationship (5) is considered (see Figure 6), that is, higher mortality is usually associated with both very high and very low temperature (stimulus) values (Baccini et al, 2008). The minimum and shape of the parabolic function, or in other words, the temperature associated with minimum mortality informs on the adaptability of a given population to the average climate.

It is important to note that heat-related mortality is strongly influenced by factors such as demographic profile of the population, warning system efficiency, health care infrastructure and air pollution (Hajat et al, 2010), and all of these are reflected in the data used to derive the impact function. In particular it is relevant to point out that in case of heat-mortality concave relationships (4) can also be found.

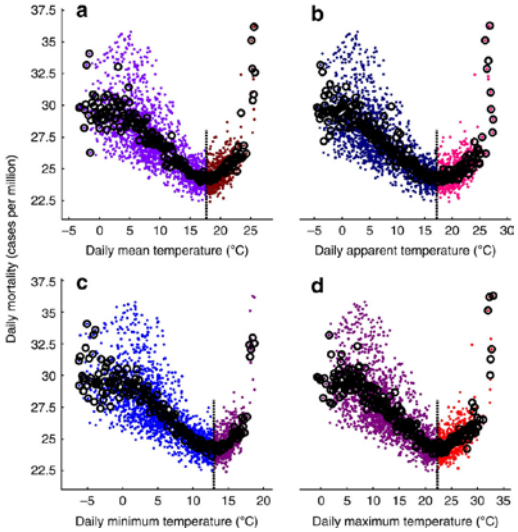

Figure 6 - Observed relationship between daily temperatures and numbers of deaths in Europe. Dots depict the daily observed values of (a) mean, (b) apparent, (c) minimum and (d) maximum temperature (°C) and mortality (cases per million) for the 1998–2003 period (from Ballester 2011).

b) Damage functions in Integrated Assessment Models (IAM)

In IAMs, damage functions are used to link macroeconomic variables (Bosello and Roson, 2007) to climate indicators (e.g., average air temperature). These functions are being used in economic analysis to estimate the risk of damage as a result of climate change. Economic climate damage is frequently analyzed using (economic) integrated assessment models expressed as the fractional loss in annual economic well fare measured by, for example GDP. Such assessments are mainly done at national, continental or global level over long time periods (e.g., a century, see Warren et al. 2006; Füssel 2010; Mastrandea 2010). Although the risk from climate damage may become increasingly significant with time, say beyond 2030, the irreducible uncertainties of future climate change decrease confidence in the quantitative results (see Covington & Thamotheram, 2015). Several IAMs incorporate two types of damage functions (market and non-market damages, see Ortiz and Markandya, 2009). Most IAMs assume and optimal implementation of adaptation, that is, that adaptation promoting actors have perfect foresight of climate impacts and that countries and regions are not constrained (e.g., financial, knowledge, institutions) in their capabilities to implement adaptation. This common approach can lead to considerable regarding the economics of both adaptation, impacts and by consequence mitigation (Patt, 2010). Sectors and impacts often incorporated include agriculture, health, sea-level rise, flooding, non-market damages and catastrophic damages.

The parameterization and form of the economic damage functions are still often based on short time series of available damage data and limited understanding of the attribution of damage to climate change versus other causes. An initial hypothesis suggests that the costs of damages increase more than proportionately with warming temperatures (convexity in damage function: see Stern, 2006), as in function 4 in Figure 1). Interestingly, the curves do not assume a levelling off in the far future, a feature that seems logical for damage at specific

locations on the shorter term where the amount of people and economic assets is bounded. The IAM such as DICE, FUND and PAGE, developed in early 90s, are still being used, for example for estimating social costs of carbon in the Stern (2006) review, and Obama's climate policy proposals (IWGSCC, 2010), and for assessing global aggregate impacts and social cost of carbon in the Fourth IPCC Assessment (Arent et al., 2014). The outcomes of these studies depend heavily on the selected discount rates and the assumed shape of the damage function. The shape of the damage function is particularly critical for projections that require the extrapolation of the impacts beyond the observed range.

As to attribution of economic damage to climate change, IPCC concludes that "*although there is limited evidence of a trend in the economic impacts of extreme weather events that is consistent with a change driven by observed climate change, climate change cannot be excluded as at least one of the drivers involved in changes of normalized losses over time in some regions and for some hazard.*" (Cramer et al, 2014). IWSGSCC (2010) observes that "*representations are incomplete and highly uncertain. But given the paucity of data linking the physical impacts to economic damages, we were not able to identify a better way to translate changes in climate into net economic damages*". One can look at this negatively, and argue that "*despite the fact that this function is key in determining results in many integrated assessment models, it is not typically calibrated in a consistent and rigorous way*" (Bosello and Roson, 2007). IAM damage functions do not have strong empirical foundations (Pindick et al., 2013). Despite this drawback, the models making use of such functions are used to infer on the future and test the consequences of logic assumptions (Stern, 2006).

c) Summary

Table 1 summarizes the main characteristics and uses of the different shapes of impact functions highlighted in the sections 2a to 2b. In general, it can be said that functions describing the relationship between climate-related impact and climate stimulus for the case of Tier 2 and 3 indicators fall within one of the five basic shapes: linear, concave, convex, s-shape and u-shape (see Figure 1). The convex, linear and concave shapes can be interpreted as sub-sections of the s-shape curve. Accordingly, the s-shape curve appears to be a good starting point to initiate the search for a functional relationship between climate stimulus and impact. The difficulties with this type of curve arise in the estimation of maximum and minimum climate thresholds for impacts, and also in the identification of which section of the s-shape curve the recorded impacts reflect.

A linear relationship between impact and climate stimulus has been observed for the cases of forest fires and agricultural production. Despite the easiness of parameterization, a linear shape falls short in describing biophysical constraints related to the impact it tries to describe. For example, while it is true that increases of temperature might favor the growing season of some species, a continuous increase of temperature will in the long run bring crop yields down. Accordingly, Mendelsohn et al 2001 proposes the use of inverted u-shape curves between crop response and temperature to reflect theoretical and empirical findings, that is:

crops respond positively to increases in temperature until an optimum is reached and declines thereafter. A similar rational is implied in the use of a u-shape curve to describe the relationship between air temperature and mortality/morbidity. In this case, the minimum of the u-shaped curve highlights the temperature value for which the lowest mortality is recorded.

Table 1 - Summary table of investigated shapes of impact functions.

Shape of the climate-impact relationship	Description	Uses	Authors	Comments
Linear	Impact increases at a constant rate with each incremental unit of climate stimulus.	Forest fires and weather variables. Crop yields and annual variability of precipitation.	Carvalho et al, 2008 Pausas 2004 Revadekar 2012	Simple to establish. Does not account for the possibility of impact saturation at high levels of climate stimulus nor for lower thresholds of climate stimulus before the impact takes place. Important to specify validity range
Concave	Impact increases faster for low values of climate stimulus, and stagnates as it reaches higher values.	Relative damage to buildings and flood height. Rice yield and seasonal precipitation/rainy days.	Boettle et al 2011 Preethi & Revadekar 2013	Accounts for the possibility of impact saturation for high levels of climate stimulus. Asymptotic upper bound.
Convex	Impact increases slowly for low values of climate stimulus and accelerates as it approaches higher values.	Relative damage to buildings and flood height. Global damages and temperature.	Merz et al 2010 Nordhaus 1992 Weitzman 2010	Impact increases indefinitely and ever faster with each increment of climate stimulus. No upper bound, asymptotic lower bound.
S-shape	Impact increases slowly for low values of climate stimulus, increases for intermediate values of climate stimulus and stagnates as it reaches higher values.	Wind speed and ratio of economic losses. Mortality and water depth.	Boyd et al. 2005 Prahl et al. 2012	Implies determining, or assuming, both a lower and an upper bound for impacts.
U-shape /inverted U-shape	Impact decreases for increasing values of climate stimulus until a minimum is reached. Thereafter the impact rises with increasing values of climate stimulus.	Air temperature and mortality/morbidity. Temperature and crop response.	Baccini et al, 2008 Mendelsohn et al 2001	Implies the existence of a minimum (u-shape) or maximum (inverted u-shape) value of impacts for a given climate stimulus.

It is important to notice the mathematical formulation of these curves can be diverse and will depend on the data at hand to establish the functional relationship and the objectives of the study, e.g., future projections of impacts vs reproduction of past trends.

3. Two approaches for indicators using impact functions in CLIPC

Sub-sections a), b) and c) in section 2 highlighted several examples of the use of empirical impact functions in regional assessments and the use of impact functions in the broader

context of IAMs. Impact functions are being developed and used across a variety of research fields ranging from those looking at physical impact, economic losses and human casualties. The strategies for developing impact functions are very much determined by the nature of the impact itself and the existence and quality of consistent observations of the impacts the function is supposed to inform about. When the losses, damages and impacts are not systematically recorded, the statistics can be insufficient to derive or calibrate impact functions (see the particular case of historical hurricane flood events in Boyd et al, (2005) in Figure 5). Additionally, the correlations between impacts and the chosen explanatory variable might be weak, so that the expected impact and its uncertainty can have a similar order of magnitude.

Despite these difficulties it seems feasible to make use of impact functions to provide meaningful information about the impacts that climate change can have. The European Commission in its call text for the CLIPC project explicitly asked for functionalities to "build" new indicators, which CLIPC has translated into the development of higher Tier from lower Tier indicators using impact or damage functions. The development of impact functions in CLIPC may improve the damage functions used in IAMs, in particular with respect to the shape of the damage curve for specific types of climate risks in different contexts.

Two basic approaches for deriving impact indicators based on empirical impact functions are proposed. The core lies in a statistical relationship (model) that links the climate signal to the impact. Given that there are multiple ways of carrying out the statistical analysis, this deliverable only sketches the main elements of the analysis (Figure 7). The determination of actual additional indicators will depend on the specificities associated with the impact that one tries to capture. The use of the two approaches in deriving three different indicators is illustrated in section 4.

The first approach (approach 1) requires that first a pre-selection of Tier 2/3 impact to be investigated takes place, together with the identification of Tier 1/climate variables (named as stimuli in Figure 7) to be correlated. Secondly, it needs to be decided on the shape of the impact-stimulus relationship. The choice of the functional form is conditional to a number of factors shown in in section 2. Once the choice of the functional form is made the next step is to fit the selected shape to the combined distribution of impact and stimulus/i. This involves the determination of parameters that minimize the error of the fit. For the simplest case (linear) the parameters involved are the intercept of the function with the x-axis and its slope. The final step is to provide the spatial distribution of the impact according to the established relation.

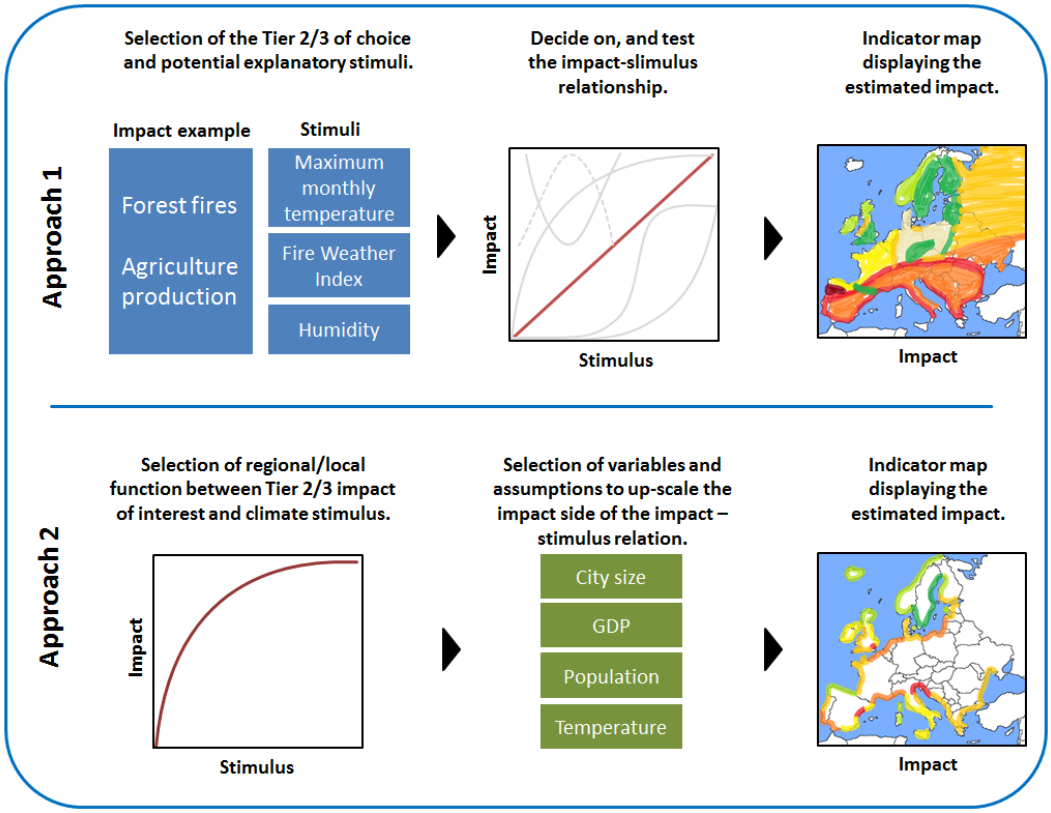

Figure 7 - Approaches followed in CLIPC for the derivation of indicators based on impact functions.

Given the scarcity and lack of consistency of observational data on impacts, robust statistical analyses across large spatial scales (e.g., continent) may not always be possible. In these cases, a complementary approach (approach 2 in Figure 7) can be used. This approach relies on generalizing impact functions published for a specific location to broader spatial scales. In the core of this approach is the definition of common variables and rules for transposing the original impact function to other spatial locations based on auxiliary information (variables).

Accordingly, the first step of approach 2 is to select an impact function that has been published and whose scope is mostly local or regional. Subsequently, it is required that a set of assumptions are employed in order to make the application of the function meaningful at a wider scale. This can be done for example by weighting the impact side of the impact-stimulus relation by the GDP, population or city size. The choice of the variable and rules is of course conditional to the impact and data availability. Finally, the indicators produced via the two approaches have to be compared to similar published work in order to assess their validity.

The heterogeneous nature (climatic, social, and economic) of the data required to create an impact function unavoidably leads to diverse sources of uncertainties that affect its robustness. It is therefore necessary to systematically examine the sources of uncertainties. In the following descriptions of impact functions and indicators (Section 3) the uncertainties have been identified and characterized and known limitations documented. Where possible a

qualitative description of confidence has been given. The uncertainty scheme is explained in Table 2. The scheme builds on work from the uncertainty assessment carried out in Task 4 of WP8 (see Milestone 37).

Table 2: General scheme for the qualitative assessment of uncertainty for Tier 2 and 3 indicators taken from work in Task 8.4

Source of uncertainty	Method to quantify uncertainty	Does this source originate rather from 'incomplete knowledge' [1] OR 'predictability' [2]?	List of known limitations and judgment on their influence	Qualitative description
This column describes the sources of uncertainties	Here are the methods listed to assess the uncertainties.	[1] '*Incomplete knowledge*' arises from the imperfection of our knowledge. It concerns what '*we do not know*' at this moment but might know in the future if sufficient time and resources are available to perform additional research or collect more data. For instance, models could be improved by adding additional processes or data might be imprecise but could be improved by more accurate measurements. '*Incomplete knowledge*' is therefore reducible. [2] '*Unpredictability*' is caused by the inherent chaotic or variable behaviour of, e.g. natural processes, human beings or social processes. It differs from '*incomplete knowledge*' because it concerns what '*we cannot know*' and therefore cannot be reduced or changed by further research.	A list of know major limitations that influence the uncertainty.	Here is given a qualitative expression of confidence, or lack, in any analysis based on the quality of the underlying evidence, possibly expressed using this scale: high: we understand the underlying processes, we can give good numerical assessments, strong evidence in multiple references. We used state-of-the-art methods to calculate the indicator (i.e. an ensemble of climate simulations, in the case of impact models, an ensemble of impact models) medium to high: we are reasonable confident in our analysis, evidence provided in moderate number of references. We used widely accepted methods to calculate the indicator (i.e. we used an ensemble of climate simulations, but only one impact model). low to medium: new evidence could have a substantial impact on our assessment, although no major surprises are expected. Evidence in a small number of references. We used less accepted (or former pioneer) methods to calculate the indicator (i.e. we used more than one climate simulation). low: we have very limited understanding of the processes or possibilities. Resilience to unexpected occurrence is called for. Evidence provided in unpublished (unverified) reports or few observations. We used a controversial method for the calculation (i.e. only one climate simulation).

In this deliverable, the two approaches are illustrated with ongoing work on additional indicators being developed in WP7. These are: a new **moth phenology indicator** based on observations of peak flight dates of several moth species; **estimate of temperature-mortality thresholds of human population** based on the correlation of minimum mortality temperatures obtained from a meta-analysis of 23 epidemiological studies; and **economic damages associated to coastal flooding** based on regional damage functions at land-use level for the entire European coastline.

Although the approaches for determining the additional indicators using impact functions are valid at the spatial scale for which data is available, the generalization may not be fully straightforward. For example, in the case of **moth phenology indicator** the results are representative for Finland only, but the statistical modelling and the combination of different types of data, including space borne data, can be applied for similar cases that link the phenology of species to climate stimuli. The other illustrative indicators are European in scope. The **estimate of temperature-mortality thresholds of human population** indicates the present capacity of the population to sustain health, while the **economic damages associated to coastal flooding** has a more prospective look on estimating economic impacts into the future. The examples have been chosen to illustrate different types of impacts and impact functions. The lessons learnt therefore have wider application in efforts to develop new indicators for Tier 2 and particularly Tier 3.

4. Examples of additional Tier 2 and 3 indicators in CLIPC

4.1 Rural theme

d) Moth phenology indicator (MPI)

We start with the example of a case in which an indicator was produced by establishing an empirical relationship between a set of climate and climate-related variables and an impact (Figure 7, Approach 1). The impact in this particular case is moth phenology, or in other words, their periodic life-cycle events. The leading question is: *Can moth phenology be predicted on the basis of variables, such as climatic (e.g. thermal sum) and remotely-sensed (e.g. snow melt, photosynthetic activity of vegetation) variables?* In practice, the indicator highlights possible changes in the phenology, measured as peak flight of moth species, which is assumed to be sensitive to climate and climate-related variables.

In order to shed some light on the question, a functional relationship has to be established between impact (moth phenology) and stimuli (climate and climate-related variables). For representing the impact side the **timing of the peak flight period** was selected. Representing the stimulus side is a set of climatic and climate-related variables to be tested such as **latitude**, **daily accumulation of thermal sun** or **date of snow melt**. Figure 8 illustrates the overall steps and data sources used for determining this additional indicator for five selected moth species representative for the Finnish moth biodiversity.

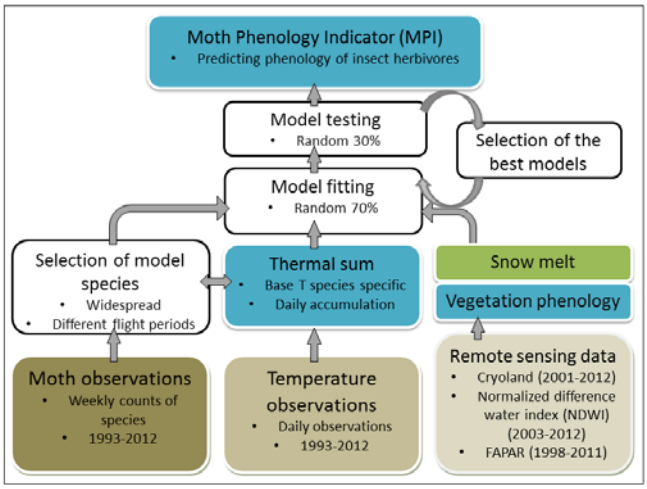

Figure 8 - Flowchart of datasets used and analysis steps conducted for deriving Moth Phenology Indicator (MPI).

Description of the approach and results

It is assumed that the relation between the occurrence of peak flight of moth species and the variables to represent the stimulus side is linear (see Figure 1, curve 1). For example, that peak flights will take place earlier at lower values of climate-related stimuli latter at higher ones.

1. **Moth observations data** - The observations of moth phenology gathered through the Finnish national moth monitoring scheme (*Nocturna*) constitute the basic phenology data for the index. Moths are observed using light traps that are equipped with mercury bulbs and run every night from the early spring to the late autumn. The traps are usually emptied and the moth specimens identified on a weekly basis. During the period 1993–2012, altogether 208 trap sites were included in the monitoring network from which 51 traps with the least temporal gaps were selected for data extraction.

   Moth species were selected for modelling based on the following criteria: wide distribution area, high abundance and timing of the spread in peak flight period during the warm season. The selected five focal species are: *Orthosia gothica* (family *Noctuidae*, peak flight in late April – early May), *Ectropis crepuscularia* (*Geometridae*, late May – early June), *Cabera exanthemata* (*Geometridae*, late June – early July), *Dysstroma citratum* (*Geometridae*, mid-August) and *Operophtera brumata* (*Geometridae*, late September – early October).

   Peak flights were selected to represent timing of the flight periods because they are less affected by inter-annual abundance variation than other descriptors of the flight period such as start, end and length. Peak flights were calculated based on the median occurrence of individuals per year and trap site. Mid-day of the median observation period is used as the peak flight date.

2. **Explanatory variables** – A number of independent variables have been used to correlate with the moth phenology data from sept 1 comprising temperature observations, remote sensing data and basic geographic parameters. **Latitude**, represented by the y coordinate of the Finnish national uniform grid system (YKJ) is used to account for a potential latitudinal change in timing of the peak flight. Temperature observations of daily mean temperatures obtained from the Finnish Meteorological Institute (Venäläinen et al. 2005) are used to determine **Daily accumulation of thermal sum,** starting from 1st January, was calculated for each 10-km grid square across Finland for the period 1993-2012. Thermal sums were calculated using 16 different base temperatures between -5 and 10 °C with intervals of one degree following previous modelling studies on moth phenology (cf. Valtonen et al. 2014). Remote sensing data was used to derive values of **Date of snow melt** in the spring for each trap site. Data was taken from the time series of daily Pan-European Fractional Snow Cover product from CryoLand (Copernicus Service Snow and Land Ice, http://www.cryoland.eu/ available for the years 2001–2012). A particular method for extraction of melt-off day despite the data gaps (due to cloudiness that prevent the observations) was developed at SYKE. **Date of greening of the vegetation** was derived from time series of the Normalized Difference Water Index (NDWI) for each trap site following the method of Delbart et al (2005). These data are available for the years 2003–2012. **Dates of start, peak and end of growing season** based on Fraction of Absorbed Photosynthetically Active Radiation (FAPAR) were derived for each trap site.

3. **Multivariate regression analysis -** Peak flight date of each focal moth species was related to explanatory variables using linear mixed effect models (lme) as implemented in the nlme library (Pinheiro et al. 2014) within the R statistical environment (R Core Team 2014). Models for species having their peak flight between the spring and mid-summer (*Orthosia gothica*, *Ectropis crepuscularia* and *Cabera exanthemata*) include **Latitude**, **Daily accumulation of thermal sum** and **Date of snow melt** and **Greening of the vegetation** as explanatory variables. **Daily accumulation of thermal sum** with a base temperature showing the lowest Akaike Information Criterion (AIC) was selected for use in each respective model. Models for the two species having their peak flight in late summer and autumn (*Dysstroma citratum* and *Operophtera brumata*) are still being developed and the results are not yet included in this deliverable. The model will include the variables of **Latitude**, **Daily accumulation of thermal sum** and dates **Dates of start, peak and end of growing season** as derived from FAPAR. For the investigated species, moth observation data was randomly divided into two sets: model fitting (70% of the data) and model testing (30%). This was done in order to allow for independent testing of model performance (predictive power). Predictive power was calculated as the proportion of explained variance (R^2) in the model testing part (30%) of the data.

Results

In Table 3 the predictive power (R^2) of total models (i.e. including all four explanatory variables) calculated for the three species having their peak flight between the spring and mid-summer (*Orthosia gothica*, *Ectropis crepuscularia* and *Cabera exanthemata*) is presented. The obtained R^2 for the total mode varied between 0.75 and 0.80 (see Table 3). In models including only one explanatory variable at a time there was large variation in predictive power between species and variables. In the early spring species (*Orthosia gothica*) all four variables showed a reasonably high predictive power, with snow melt date being the highest. In contrast, in the two species flying in the late spring and mid-summer (*Ectropis crepuscularia* and *Cabera exanthemata*) accumulation of the thermal sum appeared to determine the peak flight timing, whereas remotely-sensed variables and latitude had low predictive power.

Table 3 - Predictive power (R2) of modes for the peak flight date in the model testing part of the data (30%).

Species	Total model (all variables included)	Latitude	Daily accumulation of thermal sum	Snow melt date	Greening date
Orthosia gothica	**0.75**	0.50	0.61	**0.62**	0.57
Ectropis crepuscularia	**0.80**	0.06	**0.74**	0.13	0.20
Cabera exanthemata	**0.78**	0.03	**0.68**	0.03	0.04

It was possible to infer on the spatial prediction of the timing of peak flight periods on the basis of these models. To exemplify this approach, we have produced a spatial prediction for *Orthosia gothica* covering entire Finland and adjacent areas in Figure 9. Examples of similar spatial predictions would also be possible to include in the forthcoming CLIPC portal.

The predictive ability of different variables strongly depends on the species. For example, in the spring-flying species remotely-sensed variables show high predictive power, whereas for two others the thermal sum worked better. Remotely-sensed variables (date of snow melt, greening of the vegetation) are easily available over large geographic areas are thus good indicators for the occurrence of species active in spring and early summer, but not for species occurring in mid-summer. Finally, the spatial model predictions can be used as an interactive tool to illustrate how varying predictor values affect the phenology.

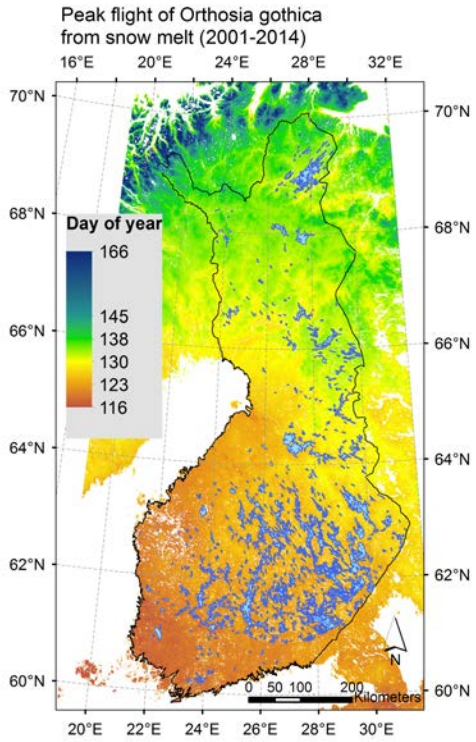

Figure 9 - Predicted peak flight date of *Orthosia gothica* during the period 2001-2014

Potential applications and uncertainties

The main potential application of the indicator can be found in its ability of predicting the timing of peak flight periods of moths on the basis of temperature observations and satellite data. The indicator has potential for application for other insect groups and extension to other geographical areas within Europe. The indicator enables the effective use of remotely-sensed variables (snow melt, greening) over large geographic areas in explaining phenology and occurrence of species, when species-specific autecological[6] patterns (such as timing of flight period, here spring – early summer only) are taken into account. There are potentially also widespread practical applications e.g. in the management of populations of insect pest species.

The main uncertainties occur in the process of deriving the different variables used in the predictive models and are documented in Table 4. Moth phenology data are collected with the resolution of one week. There are also inherent uncertainties in deriving the remotely-sensed variables of the timing of natural events such as snow melt and greening of vegetation. For example, the recent study at SYKE (Metsämäki et al. 2015) indicates that in Finland, the bias of melt-off day when compared to the in-situ snow observations is -1 day (remote sensing product is delayed for 1 day on average). The accuracy of the estimated melt-off day is lower in mid-latitude areas that only have intermittent snow cover.

[6] Autecology - The branch of ecology that deals with the biological relationship between an individual organism or an individual species and its environment.

Table 4 - Qualitative uncertainty assessment from the moth phenology indicator (MPI)

Source of uncertainty	Method to quantify uncertainty	Does this source originate rather from 'incomplete knowledge' [1] OR 'predictability' [2]?	List of known limitations and judgment on their influence	Qualitative description
Moth phenology data	Moth phenology observations are collected using an average 7-day observational period. Length of the period (in days) can be used as a measure of uncertainty.	'Incomplete knowledge' because the observational period cannot be shorter than 7 days for logistical reasons.	Observational period longer than one day causes uncertainty in the response variable of the phenological models.	Medium: uncertainty due to the length of observational period can be computed for each observation but currently it cannot be included in the predictive phenological models.
Latitude	Latitude of each trap site is presented as the y-coordinate of the Finnish national uniform grid system (YKJ). Y-coordinate of the trap location is given in metres (m)	'Incomplete knowledge' as there is a small measurement error in GPS equipment.	Locations of the moth have been measured using GPS equipment which typically have a measurement error of a few metres.	High: spatial error due to GPS measurements is very small compared to the scale of phenology models and its impact on the model predictions may be considered negligible.
Uncertainty in climate indicators	Calculations are done with interpolated daily station data on a 10 km x 10 km grid. The gridded temperature data represents the mean altitude in a grid cell. However, the locations of moths traps can be at different altitudes or could be influence by microclimatic conditions not captured by the gridded data. Some information about the interpolation error for the temperature grid exists. This has not been carried through to the actual climate indicators (thermal sums for different thresholds).	'Unpredictability' as there is some inherent uncertainty in the methodology of deriving the gridded temperature data on the basis of existing weather stations and matching these to the locations of the moths trap sites.	The gridded data has known uncertainties which are typically highest in areas with lower station density. The number of stations also varies in time.	High: temperature is being measured in fairly dense station network and spatial interpolation usually works well. The calculation of thermal temperature sums is also agregating daily time step temperature data, hence reducing uncertainty of single time-steps.
Snow melt date	Snow melt day is extracted from the times series of Earth observation Fractional Snow Cover (FSC) maps. The uncertainty is associated to the accuracy of the FSC maps AND the (temporal) length of data gaps in the time series caused by the cloud cover.	'Incomplete knowledge' as there are uncertainties in the Earth observation data.	The temporal length of data gaps increases the uncertainty if melting occurs within that gap-period.	Medium: depends on the cloudiness and the stability of snow season (intermittent snow and short snow peaks are not easily mapped).
Vegetation greening date: uncertainty due to data gaps due to clouds;	a) Cloud cover leads to temporal gaps in the satellite-time series. Observations during the time of the greening-up of vegetation could therfore be missing. b) Undetected clouds and mixed cloud pixel and other atmospheric effects lead to outliers and noise in the time series. c) The greening-up detection is based on an increase of the Normalized Difference Water	a)' unpredictability': in the case of optical instrument (on which the method is based on), because clouds hinder the observation of the surface. b)'incomplete knowledge'; c) 'Incomplete knowledge'	The temporal data gaps increase uncertainty if the greening up occurs within that gap-period. The real greening-up could occur earlier or later than satellite-derived greening up. Furthermore, spatial data gaps occur when time series with long	Medium to high: The method by Delbart et al. (2005) was verified against in situ phenological observation in Siberia. The observed RMSE was 6.7 days and the bias was negligible (Delbart et al. 2006. Remote sensing of spring phenology in boreal regions: A free of snow-effect method using NOAA-AVHRR and

	Index after snow melt in spring. In high northern latitudes snow melt and greening-up may occur at the same time. In this case the retrieved greening-up would be too late. a) The number of missing observation due to cloud cover can be quantified an included in uncertainty assessment. Time series with long gaps (<14 days) within the period of green-up are excluded for extraction of greening-up. b) Outliers can be detected based on statistical methods and removed from the time series. The noise level in the Normalized Difference Water Index time series can be assessed during the period with minimal changes in phenology and without snow cover. The noise level is considered as a relative threshold value in the retrieval algorithm. c) Additional data (for example from web-camera observation) could be used to verify in specific locations.		temporal gaps are excluded from retrieval of greening date. Sea/lake and urban areas are excluded from the detection. Due to mixed signal in the satellite pixels the greening date is not provided for areas close to lakes/sea.	SPOT-VGT data (1982-2004). Remote Sensing of Environment 101: 52-62.). We evaluated the retrieved greening dates with in situ observations in Finland and obtained an RMSE of 7 days and a late bias of 2 days (N=24). It has to be noted that phenological in situ observations are carried out on a few number of trees, whereas the observed greening date indicates greening up of all vegetation within a satellite pixel.
Modelling uncertainty	Correlations between moth phenology and climate or satellite-based indicators are not perfect, as there are other (biotic and non-biotic) factors influencing the phenology. There is some uncertainty inherent to statistical modelling methodology. Standard errors (SE) of the model parameters are used to quantify the uncertainty.	'Unpredictability' because the type of uncertainty is due to statistical modelling methodology.	There is some uncertainty affecting the model parameter values but this can be quantified using the standard error values.	high: the uncertainty connected with statistical models is well described in the literature and it can be quantified.

Potential use in the portal

Inclusion of the Moth Phenology Indicator (MPI) allows a user of the portal to explore how varying values of different variables affect the timing of peak flight periods of moth species. Models showing the highest predictive power may be used for each species in question, and the variables include accumulation of thermal sum (growing degree days) and date of snow melt and greening of vegetation. The variation in variable values will correspond to that observed during the modelling period 2003-2012. Potentially the indicator could be calculated “on-the-fly” using regularly (e.g. annually) updated data for the satellite and temperature-based explanatory variables.

4.2 Urban theme

e) Estimates of temperature-mortality thresholds in Europe

A second example on how a statistical relationship (see Figure 7, Approach 1) can be established between an impact and a set of climate and climate-related variables focuses on the urban theme, more specifically, on the threat of heat-stress to the human population of cities. This indicator illustrates approach 1 and focuses on taking heat-mortality threshold temperatures determined in peer-reviewed case-studies and correlating these with, Tier 1 indicators such as mean monthly temperatures, yearly amplitude or temperature of the hottest month and others that can be linked with city-specific threshold of air temperatures above which the excess mortality begins to rise.

Description of the approach and results

It has already been noticed in previous research that the population living in location with warmer climate in Europe poses in general higher temperature-mortality thresholds (Baccini et al, 2008), but the quantification of a response function between climate and temperature-mortality thresholds for Europe does not yet exist.

It is assumed that the relation between the threshold-temperature derived in mortality studies and climatic variables representing the long-term climate characteristics follows an S-shape curve (see Figure 1, curve 3) relation implies the existence of a minimum and maximum range for impact. In other words, stimuli values beyond which the maximum and minimum impact stagnates. This work establishes a multivariate regression between a range of literature-derived city-specific temperature thresholds and 14 independent variables that comprise climate, topographic, demographic and structural characteristics of a city.

1. **Case study selection** – We focused on single site and multilocation studies that conducted time-series regression or case-crossover analysis on daily mortality and provided an absolute threshold temperature in one of the following units: mean temperatures (T_{mean}), mean apparent temperatures (defined as: perceived outdoor temperature, caused by the combined effects of air temperature, relative humidity) ($T_{mean\ apparent}$), maximum temperatures (T_{max}), maximum apparent temperatures ($T_{max\ apparent}$). Data on threshold temperatures, observed time frames, and if given, summer months, mortality causes and age stratification was gathered from the studies. Thresholds for the same day temperature exposure, that is, at lag 0 were used. In case these were not available, thresholds for the following day (lag 1) were used. In case of multiple studies by the same author observing the same cities and time frames, only one study was considered in order to give each city and observed time frame the same weight. Some cities appear multiple times due to their occurrence in more than one study, amounting to N=96 cases observed. These cases are found to be distributed as shown in Figure 10. Mostly cases are in Europe, North America and East Asia, with less cases in South America, the Middle East and South Asia and Australia. Most of the threshold temperatures collected are given in T_{mean} (about 60 of the 96), followed by $T_{mean\ apparent}$, T_{max} and $T_{max\ apparent}$ (see panel b) of Figure 10).

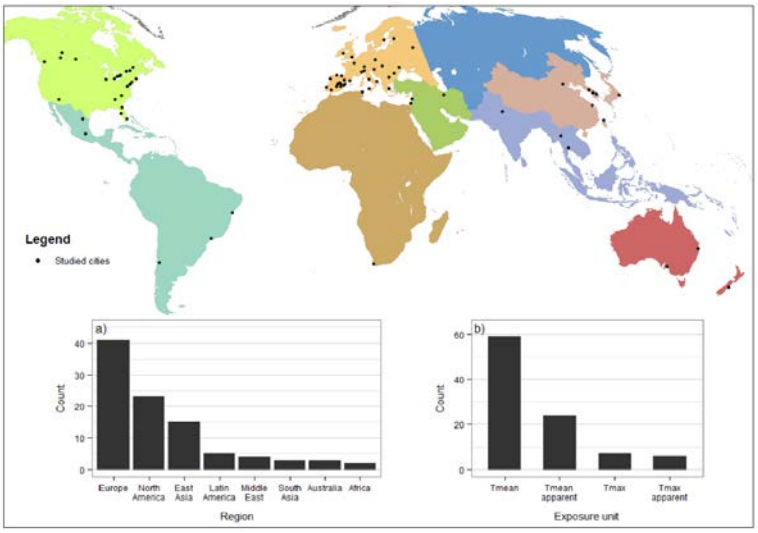

Figure 10 - Spatial distribution of cities from which threshold temperatures are investigated and the distribution of threshold temperature units in the considered studies.

2. **Conversion of temperature-mortality thresholds** – Given the diversity of temperature aggregations (e.g., daily mean temperature, daily mean apparent, maximum daily temperature, and maximum apparent daily temperature) in which threshold temperatures can be expressed (see step 1), a homogenization procedure to convert threshold temperatures to a common unit is required. Figure 11 illustrates how the conversion of threshold temperatures to a common unit was undertaken. Climate data from stations located within 10 kilometer buffer around each city was extracted from the Global Summary of the Day (GSOD), Version 7 by NOAA's National Climate Data Center[7]. Stations with data covering time series with less than five years where excluded unless they complemented data of time series of stations nearby. The number of stations representing a city's climate varies across the study cities between one and six.

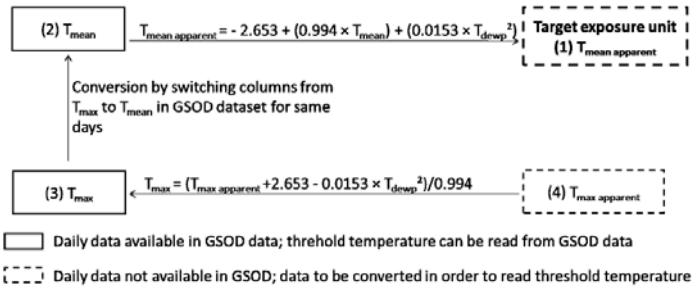

Figure 11 - Conversion paths to homogenize threshold temperatures across the investigated studies.

[7] Available at: http://www7.ncdc.noaa.gov/CDO/cdoselect.cmd?datasetabbv=GSOD&countryabbv=&georegionabbv=

Daily $T_{mean\ apparent}$ (see box (1) in Figure 11) is used as target unit as it incorporates the effect of humidity. We extracted time series from the GSOD data according to the observation period from the original study for the respective city. We identified the days corresponding to the threshold temperature obtained +/- 0.5 ºC. As GSOD temperature data was either given in T_{mean} and T_{max}, threshold temperatures provided in the apparent equivalents first had to be converted into the actual air temperature in order to match it with values in the GSOD data. The average temperature converted into $T_{mean\ apparent}$ of the days that met the threshold condition constituted the new threshold temperature. Figure 11 illustrates the conversion paths for the homogenization of original HM relationship threshold units into the target exposure unit $T_{mean\ apparent}$. Original thresholds given in $T_{mean\ apparent}$ remained unchanged. Thresholds given in T_{mean} (conf. (2) in Figure 11) were converted into T_{mean} apparent according to the top equation shown in Figure 11 from Steadman (1984). We continued the calculation into $T_{max\ apparent}$ for the respective days using T_{mean} that was given in the GSOD time series (step (3) in Figure 11). $T_{max\ apparent}$ step (4), thresholds were converted to T_{max} (3) using equation Figure 11. Having received T_{max} as a result, the threshold conversion was continued as already described above for T_{max} values.

3. **Independent variables** – Independent variables identified in the literature as influential for shaping the heat-mortality threshold were collected for the investigated cities. The variables can be divided into two broad groups, those that reflect the climate and geography of the city and those that characterize the city. The independent variable used to characterize the city's climate were: **30-year average of daily mean temperature (Tmean30)**; **30-year average of the annual amplitude (Amplitude30)**; **30-year average summer temperature (Summer30)**; **30-year average of the hottest month's temperature (Max30)**; **average temperature of winter before observed summers (Winterbefore)**; **30-year average of winter temperatures (Winter30)**; and also, **Distance to coast (Distcoast)**; **Latitude** and **Elevation**. The 30yrs time period corresponds to the 30 years before the date of the first year used in the HM study itself. The variables used to characterize the city's demography and geography are the following: **City population (Citpop), city population density, city urban extent (Citext)**; **percentage of urban cluster of the convex hull (Surgreen)** and **urban green space in percent of urban extent (Urbgreen)**. City characteristics are extracted from Version1 of the GRUMP settlement points shapefile CIESIN (2000) and Globcover[8] land cover data.

4. **Multivariate regression analysis –** The city-specific variables from step 3 are correlated with homogenized threshold temperatures resulting from step 2. A principal component analysis was carried out, considering the independent variables listed and the threshold temperatures. Based on the principal components (PC) accounting for

[8] Available at: http://due.esrin.esa.int/page_globcover.php

the largest proportion of variance, independent variables with highest factors were selected for further analysis. We establish a preliminary linear multivariate regression model to detect the variables with highest significance levels and with largest influence on the threshold temperature. We select the linear regression model according to the Akaike Information Criterion (AIC) while simultaneously considering model simplicity. **Tmean30**, **Amplitude30**, **Distcoast, Citpop** and, **Citdens** are returned as the most significant variables. When simplifying the model for the population-related variables all remaining variables are returned as significant at a level of less than 0.001 with an adjusted R^2 of 0.74, a residual standard error (RSE) of 3.4, a root mean square error (RMSE) of 3.35 ºC and an AIC of 514.5.

An s-shape function is constructed using the most significant variables as follows:

$$TM = \frac{M}{1+e^{-x}}$$

in which TM is the estimated threshold mortality, and x is

$$x = a\,y + b\,z + c\,w + d$$

in which *a*, *b*, *c* and *d* are fitted parameters, and *z*, *y* and *w* are respectively the variables **Tmean30, Amplitude30, Distcoast**. The value of M is set at 45 after a sensitivity analysis showed a stagnation of residual standard error at about 3.5 for M values beyond 45.

Results

The observed threshold temperatures (step 2) compared to the predicted threshold temperatures produced (step 4) is presented in Figure 12 (left) classified according to climate zones and humidity regimes (aggregated Köppen-Geiger system). In general the thresholds predicted by the model are in good agreement with the observations within a standard error of 3.4 ºC. In general, as can be expected logically, cities characterized by having cold and humid winters (Df) tend to cluster around the low threshold temperature ranges, whereas cities in arid steppe climates (BS) and in the tropics (Af, Am, Aw) tend to occupy the high-end of the threshold temperatures considered. Threshold temperatures in cities located in warm temperate climates, both dry (Cs) and humid (Cf), are ranked in between. Figure 12 (right) allows for the investigation of the dependency between threshold temperatures and the variables T_{mean30} and Amplitude30. The cities are ranked according to their values of Tmean30 on the x-axis and temperature thresholds on the y-axis. The size of each bubble indicates the Amplitude30 value of each city and the colour its climatic zone. It can be observed that as Tmean30 values increase, so does the average threshold temperature. The effect of Amplitude30 in driving Threshold temperatures is better observed in cities with medium Tmean30. For these, above average values of Amplitude30 (larger bubbles) are

associated with higher values of threshold temperatures. A high value of Amplitude30 alone is not associated with middle and high threshold temperatures if T_{mean30} is low. On the other hand, a high T_{mean30} value is associated to high thresholds temperatures even in case of low Amplitude30.

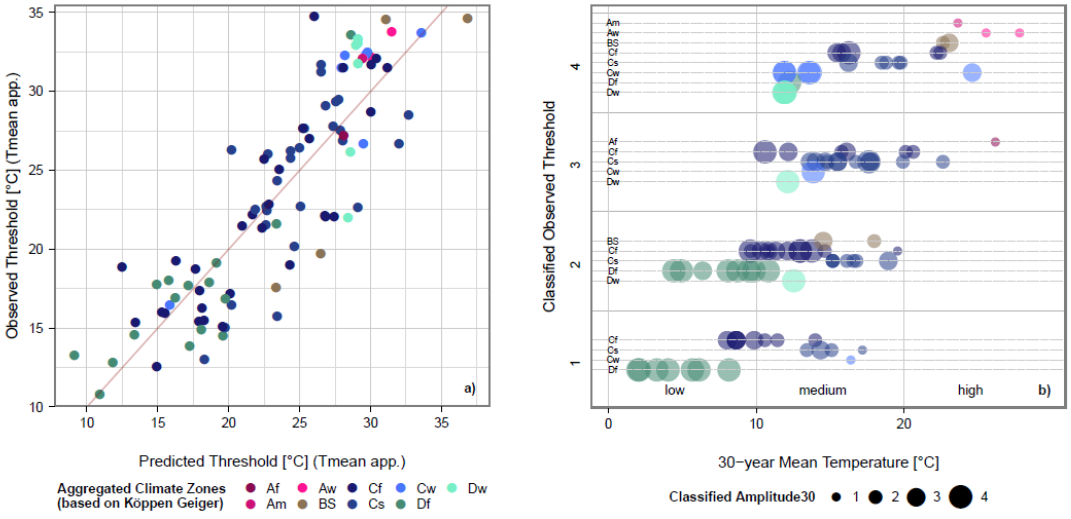

Figure 12 – Left: Observed versus predicted threshold temperatures in T mean apparent (ºC). Right: Classes of observed threshold temperatures plotted against absolute values of Tmean30 and Amplitude30.

On the basis of the empirical relationship established, it is possible to show the spatial distribution of temperatures associated with minimum mortality of the human population. The example in Figure 13 shows the results obtained for the European continent.

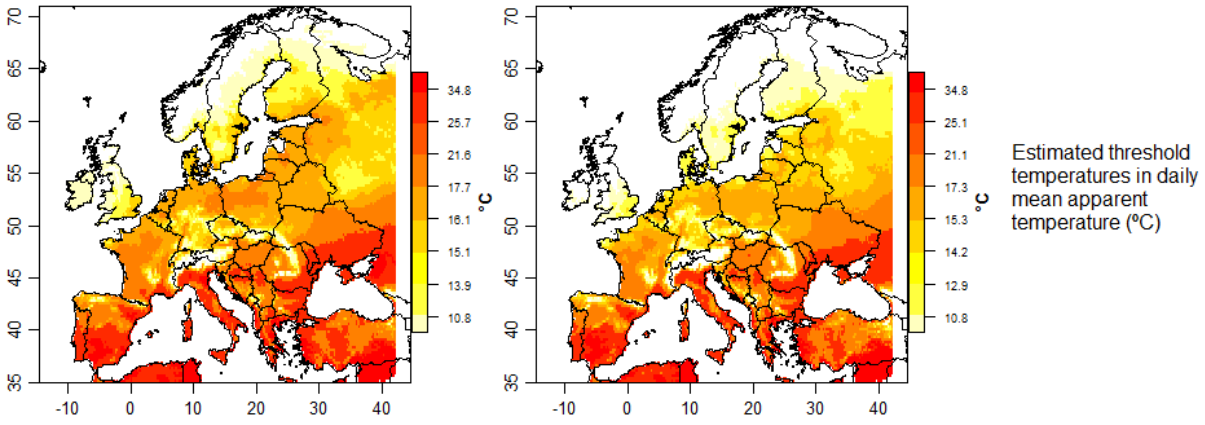

Figure 13 – Estimated threshold-mortality temperatures of human mortality in Europe following a linear model. Left: temperature classified using equal distance. Right: Temperatures classified using equal quantile method.

Potential applications and uncertainties

There are a number of possible applications for the developed indicator. First, one can assess the strength of climatic and the other variables tested in explaining the threshold mortalities observed in the city-sample, as explanatory variables. Accordingly, we found in our analysis that past climatic conditions play the (statistically) most important role in determining the level of threshold mortalities in the investigated cities. Variables like urban extent, fraction of green areas, and even population number and density, only had low predictive strength for the dependent variables investigated here. Additionally, the indicator allows better contextualizing other indicators such as number of hot days (day on which the maximum air temperature is at least 30°C). Two regions with the same number of hot days in the future but with different temperature values associated with minimum human mortality will likely exhibit also different levels of impacts on the population. The indicator can therefore be interpreted as the current level of tolerance to heat by the population.

Second, another potential application of the indicator is that it provides a first order approximation of threshold temperatures in locations where so far no specific heat-mortality study has been conducted. This might prove to be particularly relevant for the cases of developing countries where studies of this nature are rare, see also Figure 10b. In addition to the uncertainties reported in Table 5 there are uncertainties related to the actual underlying processes. For example, the observations cannot be interpreted to mean that there are large physiological differences between the people living in different temperature conditions. Instead the indicator provides a combined synthetic overview of numerous factors that influence the mortality.

Table 5 - Qualitative uncertainty assessment for temperatures associated with minimum human mortality

Source of uncertainty	Method to quantify uncertainty	Does this source originate rather from 'incomplete knowledge' [1] OR 'predictability' [2]?	List of known limitations and judgment on their influence	Qualitative description
Climate data (station) uncertainty.		'Incomplete knowledge' – Data gaps in some of the time series used as well as lack of coverage in some countries contribute for the overall uncertainty. In addition one always has to consider potential systematic errors from the measurement instruments.	Systematic measurement errors.	High – there is good confidence on the measurements.
Climate data (interpolation) uncertainty.		'Incomplete knowledge' - ridded data sets derived through interpolation of station data have a number of potential inaccuracies and errors. These errors can be introduced either by the propagation of errors in the station data into derived gridded data or by limitations in the ability of the interpolation method to estimate grid values from the underlying station network	Systematic errors on the interpolation procedure.	High – The statistical methods to interpolate climate variables are well described and associated errors documented-
Threshold temperatures reported in the case studies.		'Incomplete knowledge' - The uncertainty of the estimates is usually reported in the original study although not using the same standard. Often the threshold values are	Systematic errors on the interpolation procedure.	Medium – Not always clear the used method for determining the

	given as the 95% confidence interval and 5 % significance level.		threshold temperature. No access to original mortality data. On the other hand the studies have all been through peer-review process-
Threshold temperatures conversion.	'Incomplete knowledge'- The necessary variables for the conversion of threshold temperatures are extracted from the days in the time series which present a +/- 0.5 degree variation to the original threshold temperature. There is no way to precisely assess which days in the time series had the exact temperature as the threshold temperature reported in the study given that the datasets used are no the same.	Simplification of the conversion to Tmean apparent leads to systematic errors	Medium – The assumptions made to convert the temperatures are debatable but the equations used are well established.

Potential use in the portal

The use of this indicator in the portal would be complementary to TIER 1 indicators that inform on the potential stress of heat on human population, as it provides estimates of the current level of tolerance to heat by the population. Additionally, it can also be used to explore and evaluate regional differences of heat tolerance of populations across Europe.

f) Potential economic damages from coastal flooding in Europe

The two first examples show how additional indicators for the CLIPC portal have been derived based on a definition of an empirical impact function established between climate variables (and others) and impact. The next example will explore a case where already existing impact functions derived from regional to local contexts, are systematically employed across Europe. The indicator discussed in this section provides information on the potential economic losses at the European coast from future sea-level rise and storm surges. In this particular case the climate variable, or better, the climate-related variable is the potential flood level at a coastal location, and other independent variables relate to land use and land cover, and the dependent impact variable is expected economic damages in €/m2.

Description of the approach

For different land-uses it has been suggested that the relation between fraction of damages in case of a flood event and the inundation depth follows approximately a concave curve (Huizinga 2007) As illustration of the approach 2 in Figure 7, we apply the impact function across the entire coastal extent of Europe in order to determine the potential monetary damages associated with to coastal due to sea-level rise. The work builds upon the experience of applying the same impact function for individual cities only explored in the RAMSES project. Unlike the indicators described in the previous sections, the main challenge involved in approach 2 is to develop rules for transposing the impact side of the relationship across larger scales. The following steps describe the approach followed.

1. **Land-cover extraction** – A regular grid of 25 by 25 km was created along the coastline of Europe (see Figure 14). According to the spatial extent of each grid, Corine Land Cover (CLC) data level-3 (ETC 2013) for the years of 1990, 2000, and 2006 was extracted. Year 2006, 100 by 100m resolution. The CLC datasets map homogeneous landscape patterns, i.e. more than 75% of the pattern has the characteristics of a given land cover class. The class nomenclature is a 3-level hierarchical classification system. In its more detailed version it accounts for 44 classes.

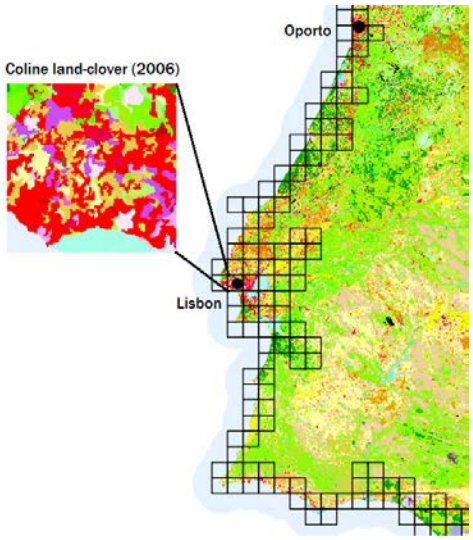

Figure 14 - Example of extracted land-cover (2006) by a regular 15km grid around the region of Lisbon

2. **Flood route modelling** - Based on EU-DEM elevation data with a horizontal resolution of 25m (DG Enterprise and Industry 2013) and a flood fill algorithm using the 8 nearest neighbors (see Boettle 2011) the flooded grid cells at a presumed flood height are determined. In addition to the information, whether a grid cell is flooded or not, also the corresponding inundation heights are recorded. This approach disregards the effect of artificial flood barriers. The procedure is carried out for all flood levels between 0 and 10m in steps of 0.5m.

3. **Inferring land-use of flooded areas** – While land-cover classes from step 1 provide the location of assets at risk, the construction of a damage function requires information of the economic value of the assets. Starting with Corine Land Cover information, we use the Land Use/Cover Area Frame Statistical Survey (LUCAS) report (EEA 2006) in order to infer the corresponding land-uses. The LUCAS report provides the empirical composition of land uses for all CLC classes in Europe. At this point, we have all physical information needed: the inundation height of each grid cell for a given flood level as well as its land use. For this work only urban land-uses are considered, given that they compose the highest share of maximum damages.

4. **Application of land-use specific damage functions** - The physical information from the previous steps is converted to monetary damages by employing relative damage functions for the corresponding land-uses (see Figure 15). Relative damage functions deliver only fractions of value lost (see also section 2). Accordingly, an estimate of the maximum economic value that can be damaged within a given land-use class is required. Values regarding this dimension are taken from Huizinga (2007) available in €/m^2 per land-use category. Using the land cover/use relation from the LUCAS report, we infer damage functions for CLC classes as composition of corresponding land use damage functions. The application of points 1 to 4 results in damage estimates in each individual CLC grid cell at a hypothetical (0 to 10m) flood level. See a spatially confined example of the results obtained in Figure 17.

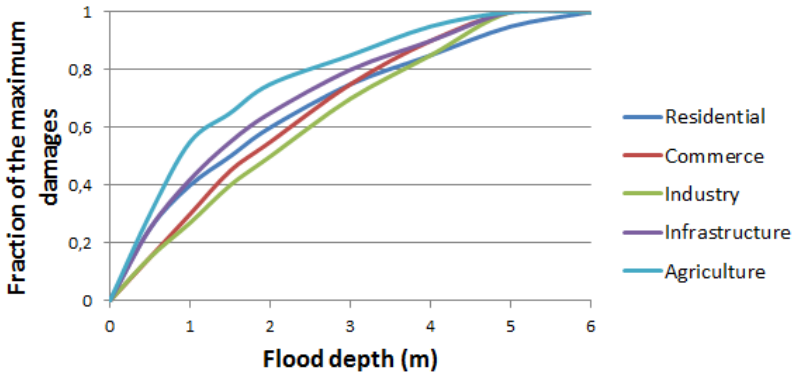

Figure 15 - Relative damage function for specific land-used from Huizinga 2007 and developed for the European context

5. **Surge heights and sea-level rise** – In order to reflect the best current knowledge on sea-level at the European coastlines, we use AR5 (Church el al, 2014) projections of sea-level for RCP's 2.6 and 8.5 determined using 21 CMIP5[9] AOGCM[10]. Storm surge levels to be included at a later stage will be extracted from DIVA v0.01 database (Vafeidis et al 2008) and linked to the long-term sea-level trends provided in AR%. The flood return levels corresponding to the 10, 100 and 1000 returning periods will be used. Although this version is by now outdated, the main advances made in DIVA have been made regarding the updating of new future scenarios and advances on the impact and adaptation evaluation. The storm surge data taken refers to the past situation and hence not expected to vary substantially in the new version.

6. **Coastal protection** – There is no consistent database on the location and protection standard of coastal defenses in Europe. As a result of this lack of information, studies evaluating the economic impact of sea-level rise and storm surges assume that the need for costal protection is a function of the economic assets at risk of being damages

[9] Coupled Model Intercomparison Project Phase 5
[10] Atmosphere-Ocean General Circulation Model

at a given storm surge return level and the costs of building a dike with a corresponding height to offset the totality of damages. Some information on current coastal protection standards is nevertheless available for cities/regions in scientific, grey literature and expert judgements (see Figure 16) but the coverage is incomplete and the methods of assessment inconsistent.

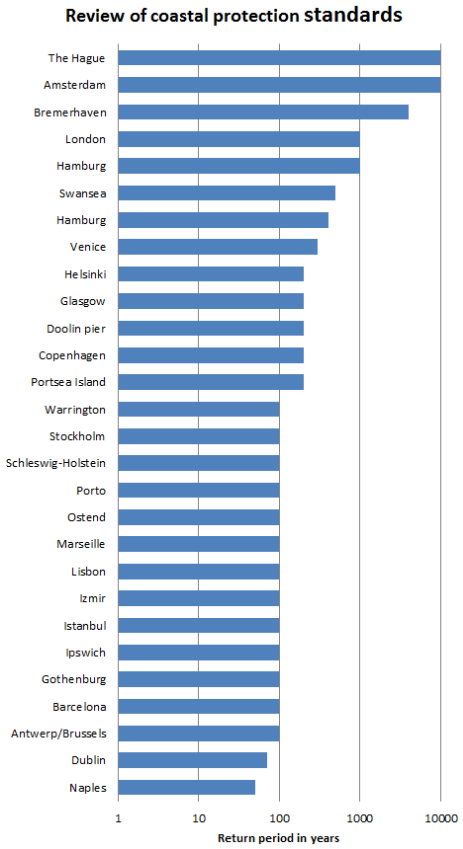

Figure 16 - Review of coastal protection standards for a collection of European cities (CLIPC work).

If information of the protection standard for a city/region was available then the most usual standard found was the 100 year return level. Only two cities (Naples and Dublin) were found to have a lower protection standard. Higher protection standards equal to 200, 500, 1000 and 10000 return level were also found. The inclusion of the mitigation effect of coastal protection is planned to be as follows: Damage is assumed to take place in a grid cell only for the surge levels return level (see step 5) which are above the coastal protection standard. The protection standard in each grid for urbanized areas is either extracted from existing literature or assumed to be equal to 100 years.

Results

A snapshot of the results obtained from carrying steps 1 to 4 is shown in Figure 17. The map highlights the spatial distribution of estimated economic damages from a hypothetical 1.5 meter flood in the city of Copenhagen in € for the year of 2014 (using land-cover data for

2006, excluding the effect of installed protection measures). The results are available in the same resolution as the land-cover input, that is, 100 by 100 meters.

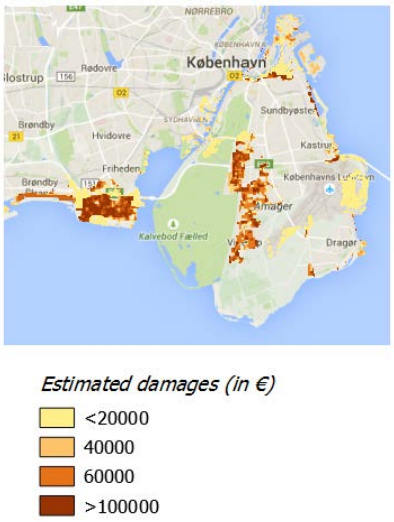

Figure 17 – Damage estimate from a hypothetical 1.5m surge for the urban land-cover classes around the city of Copenhagen using 2005 land-cover data.

Results are also available on 15km grid, in which each cell contains the sum of all damages that fall within its spatial extent. The aggregation is available for different points in time, namely 1990, 2000 and 2006. Figure 18, shows the results of steps 1 to 4 detailed in the description of the approach (see above), or in other words, the derivation of impact functions for each grid cell considered. The example below refers to the same grid cell as highlighted in step 1 containing the city of Lisbon (land-cover data used in the example refers to the year 2006). For low flood levels (e.g., below 2 meters) practically no damages are projected to take place. These start to be most noticeable for flood levels above 2 meters. Until a hypothetical flood depth of 6 meters the estimated damages increase very slowly for each additional unit of flood depth. Beyond 6 meters flood depth, estimated damages start to increase linearly, almost doubling the amount of damages by each additional meter of flood depth.

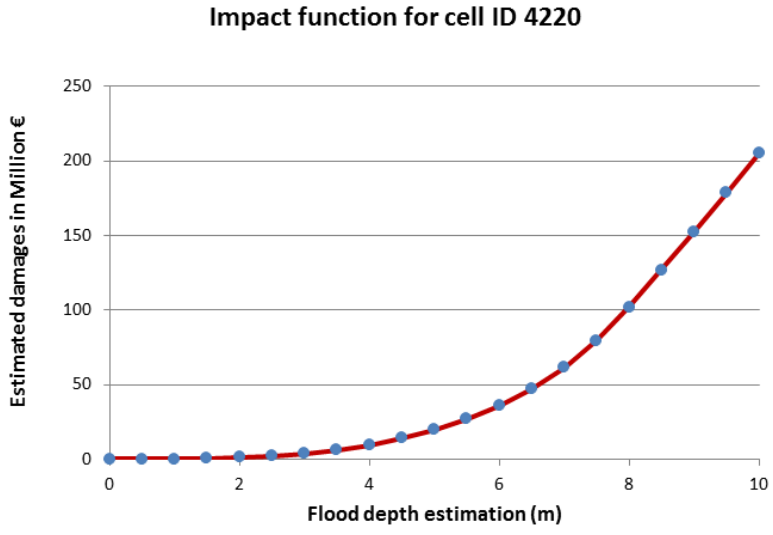

Figure 18 - Impact function for the grid cell highlighted in Figure 14.

The impact functions per each grid cell constitute the underlying data for the investigation of flood damages associated with a particular surge level. Figure 19 shows the preliminary results of the impact estimation for Europe. Impacts in Bln € have been estimated for the medium values of sea level rise resulting from RCPs 2.6 and 8.5 as given in the AR5. The next step is to include the effect of storm surge level such as those given in the DIVA model v0. The results do not yet include the effect of coastal protection or land–use changes, this dimensions still being integrated. The preliminary results show the largest estimated damages in the regions of the Netherlands, Belgium, Germany, Northern and Western France and Northern Italy. As a whole, the spatial pattern of damages appears similar to other works preformed at a comparable level of aggregation (Hinkel et al 2010).

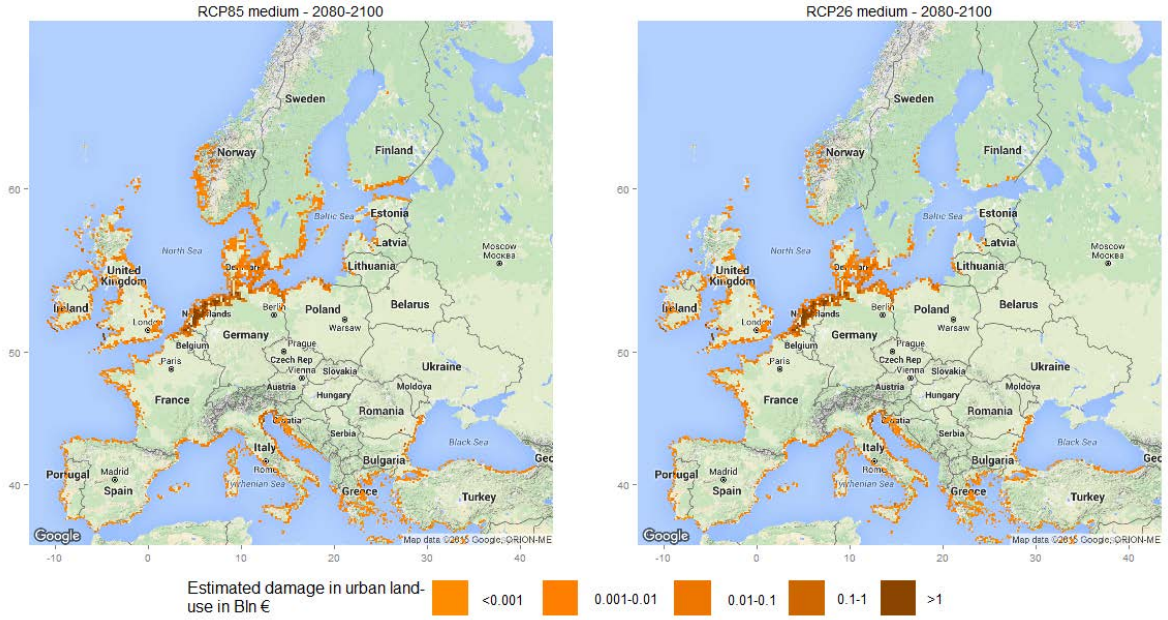

Figure 19 - Estimated impacts from progressive coastal flooding due to mean sea-level rise by 2080-2100 for two RCP scenarios, excluding the effect of coastal protection.

The statistical approach in LUCAS produces typical fraction of land-uses by land-cover for Europe as a whole. Accordingly, the method at the moment gives only a crude view on the hotspots of potential damages along the European coastline. Because the preliminary damage estimate utilized all land-cover classes as input, the scaling effect of the land-use fractions in LUCAS can become substantial for particular regions. To minimize this effect, the subsequent version will limit the damage estimate to urban land-cover only, where land-uses are potential more homogeneous between countries.

Potential applications and uncertainties

The main potential application of the indicator is the possibility of transforming location-specific surge heights into an estimate of economic damages associated with different land-uses. This differs from other approaches such as (Hinkel et al, 2014) in which number of

people living below a given elevation level and per capita GDP are used as proxy for assets. With our approach the planning of coastal adaptation measures can be done by land-use type. Additionally, the resolution of the land-use data (100 meters) is by far greater than those used in similar work (Hinkel et al, 2012). Using the empirical damage functions associated with different types of land-use and time horizons allows for urban adaptation to coastal flooding to be analysed at several levels such as actions to modify the function itself, e.g., prevention measures at the land-use scale that change the response between flood depth and economic damage (see Figure 15). Or also adaptations through land-use planning, e.g., align land-uses associated with high capital value with moderate flood depths.

Table 6 - Qualitative assessment of uncertainty for the economic damages from coastal flooding in Europe.

Source of uncertainty	Method to quantify uncertainty	Does this source originate rather from 'incomplete knowledge' [1] OR 'predictability' [2]?	List of known limitations and judgment on their influence	Qualitative description
Corine land-cover data uncertainty	Compare to alternative sources of land-use data., e.g., LANDSAT	'Incomplete knowledge' - Errors due to recent changes in land cover. Inaccuracies introduced by the classification of land-cover from satellite imagery. Additionally the dataset maps homogeneous landscape patterns, i.e. more than 75% of the pattern has the characteristics of a given class from the nomenclature.	Systematic errors. Potential overestimation of land-cover patterns.	High – CORINE land cover a well-established dataset provided by authorities sources.
Elevation model uncertainty	Comparison of elevation values with other more detailed DEMs such as for example LIDAR.	'Incomplete knowledge' - Measurement errors and inaccuracies due to spatial resolution. The dataset is a product of interpolation from SRTM90.	Systematic errors introduced in the interpolation process.	Medium – The elevation model is a reasonable approximation of the topographic features of the study area.
Flood algorithm uncertainty	Comparison of food extent and depth with outcomes of more detailed hydrological models.	'Incomplete knowledge ' - Very simplified algorithm estimates “asymptotic filling” of area. The 8-rule for flooding as described in Poulter and Halpin (2008) is applied.	Simplification leads to a systematic overestimation of the flood extent.	Medium – Although simple we have medium confidence that the algorithm is delivering meaningful results on the most risk-flood prone areas.
Land-cover to Land-use conversion uncertainty	No straightforward way to assess uncertainty.	'Incomplete knowledge' - The conversion of land-cover into land-uses is limited by the information in the LUCAS survey (see section 3.1). In the particular case of this indicator, about 20% of land-cover could not be converted to a respective land-use.	Systematic underestimation of damages.	Low – There is not much confidence om the conversion of land-cover to land-use to be meaningful for every coastal location due to the top-down approach used-
Relative damage function uncertainty	Make use of other existing relative damage functions to determine damages and assess the differences.	'Incomplete knowledge' -The same relative damage functions are used across all countries. This implies that there are no changes in the sensitivity of similar type of	Systematic error by assuming the same relative damage function for all land-uses independent of the country.	Medium – The damage functions are constructed using empirical data on economic damages but the associated uncertainty ranges are not given.

		assesses across Europe.		
Asset value uncertainty	Determine asset value at risk via alternative proxies, for example, per capita GDP or fixed capital stock.	'Incomplete knowledge' - In the absence of a consistent valuation of assets across Europe, the maximum potential damages for a given land-use in Huizinga 2007 are scaled are scaled according to the economic power of a country.	Systematic error by assuming the same value of assets in a given country. Potential over estimation of damages in the rural areas and underestimation in regions with high accumulation of capital, such as cities.	Low – There no low confidence that the approach taken to estimate asset values across countries is representative for the asset value at the coastal locations.
Sea-level and storm surge uncertainty	Use multiple scenarios of sea-level projections to obtain a range of values.	'Unpredictability' - Storm surges are stochastic events and therefore unpredictable. On the other hand, sea-level change can be anticipated with considerable robustness given the long-term physical processes involved.	Limited number of scenarios for sea-level rise does not cover the full scope of potential futures.	Medium – Process models delivering sea-level estimates are a matter on ongoing debate.
Uncertainty on existing coastal defences.	No straightforward manner to assess uncertainty.	'Incomplete knowledge' - There is no consistent global, or European, information on the current protection standard of coastal defenses, their relative height or condition.	Basic assumption that no damage occurs if surge level below or equal the protection standard might lead to ad under estimate of the real damages.	Low – There is not enough knowledge on existing protection structures, their state and protection level across Europe and our approach is greatly conditioned by this fact.

Potential use in the portal

The usage of this indicator in the portal provides the possibility for potential users to explore the economic damages in the coastal zones of Europe for particular surge levels. The spatial and temporal coverages imply that European-wide maps are possible for the years of 1990, 2000 and 2006 (and 2012 when CLC data for 2012 becomes available), although some countries might be absent in particular years (e.g., Greece 2000 and 1990). Given the relatively high resolution of land-cover datasets, damage estimates provided can be aggregated to regions of interest such as NUTS 2 level. It is not foreseen that users can modify the basic relative damage functions used (see step 4). The collection of relative damage functions used was developed within the European context and is a product of synthesis from European case studies. In this sense we assume that the relative damage functions used already represent the best current knowledge on the sensitivity of assets to flooding in Europe.

4.3 Additional options for the use of impact functions

The examples of additional indicators presented in this deliverable make it possible to reflect on further opportunities for the use of damage function in the CLIPC portal and in the production of Tier 2 and 3 indicators. Regarding the first case it can be suggested to make use of simple impact functions that support users who wish to explore the socio-economic impacts of a changing climate. For example agricultural gains/losses of specific crops can be determined using published impact functions based on Tier 1 and 2 indicators documented in deliverable 7.1, such as changes in growing season length, temperature and, precipitation. A similar case could be thought to be the impact of forest fire occurrences, which have been

reported to be significantly correlated with climate stimuli such as maximum summer temperatures or Forest Weather Indices. In the absence of a dedicated impact model to inform on the sensitivity of society and economy to climate, the elaboration of easy to grasp (although admittedly simplistic) quantifications between impacts and climate could provide a value added to users. An additional idea would be to first supply users with qualitative descriptions of possible links between climate change variables (Tier 1) and social or ecological variables, and then allow them to test visually the association between the described variables. By doing so, users would be in practice visualizing potential impact functions. Caveats would have to be spelled out clearly in order to avoid over interpretation.

The examples of indicators presented in this deliverable constitute only a fraction of a broader range of possible associations between socio-economic-ecological impacts and climate stimuli. The number of indicators could be expanded by using the two approaches elaborated in this deliverable as guiding framework for establishing impact functions across a larger suite of indicators in the CLIPC-WP7 inventory. For example: water-limited crop productivity as a function of precipitation, percentage change in arrivals/departures as a function of temperature increase, irrigation water demand as a function of dry days, energy consumption as a function of heating degree days etc.

There is a large potential in integrating consistent socio economic data from data providers such as the EUROSTAT with Tier 1 indicators and climate variables. Such impact functions could follow the two general approaches described in this deliverable as a framework for the analysis.

5. Discussion and Conclusions

Many authors have argued that the use of indicators depends critically on the indicators meeting criteria of legitimacy, credibility and salience (Bauler 2012). Climate change Tier 1 indicators, which describe the main drivers, can be highly salient in raising awareness of climate change, because it is easy to understand the general significance of indicators such as heavy rainfall, extreme temperatures or drought even without further elaboration. As they also represent a long tradition of measurements/projections, their credibility is often strong. Issues of legitimacy hardly arise, because the data are collected by a long-established and well-connected network of national (hydro-) meteorological institutions.

When it comes to taking action, especially action requiring major investments or other resources, the salience becomes more specific, with demand for indicators of the relevant impacts, and impacts and associated damage costs. As it has been noted, climate science usability is a function both of the context of potential use and of the process of scientific knowledge production itself (Dilling and Lemos 2011). Indicators can justify the action and prioritize different possible actions. There is thus a need for ‘actionable’ information and Tier 2 and 3 indicators can respond to this need. At the same time many Tier 2 and 3 indicators suffer from large uncertainties as shown by the scatter of points in the relationship between

climate stimuli and impacts, eroding their credibility. Issues of legitimacy may also arise in the choice of indicators, which are not evenly distributed over Europe and come from a variety of sources distributed over different countries and different types of organizations.

Impact functions may help to focus on the salient features of the Tier 2 and Tier 3 indicators and give better rules-of-thumb indicators than the original data on impacts. Especially long term planning is often based on broad brush information (Dunn, Lindesay, and Howden 2015) and this is what impact functions can provide. Obviously this increase in salience may come at the cost of a loss of credibility. Credibility can be lost if the chosen combination of Tier 1 indicator and impact variables (impact or damage function) is based on weak claims of attribution or if the chosen function leads to poorly justifiable extrapolations. Care will therefore have to be taken in displaying and 'marketing' impact functions and the uncertainties should be made explicit. Studies have shown that managers and planners are at ease in dealing with uncertainties, but they need information on uncertainty ranges (Tribbia and Moser 2008).

Further development of indicators can proceed in a number of ways. The most obvious route is to continue to search for statistical relationships at European scale between data on climate change impacts (for example flood damages) and climate variables as in approach 1 (Figure 7). Material available for this approach can be expected to increase with the development of, among other things, the Copernicus climate services[11]. The credibility depends crucially on the length of the available time series and the spatial extent of the data affects the salience of any resulting impact function. The generalization of localized impact functions as in Approach 2 (Figure 7) requires additional data to credibly transfer the function to areas outside the range for which it has been developed, or at least data that allows users to reflect on the robustness of the parameters in the impact functions. The analysis of heat mortality is a case in point, demonstrating the importance of context (Section 3.2). In addition to these approaches that build on data of known climate change impacts, an additional route is to use the impact function approach to explore possible climate change signals in socio-economic data that so far has been analyzed to a limited extent from a climate change perspective (Lückenkotter et al., 2015, 2016).

For policy makers socio-economic data is often highly salient. If an "impact function approach" is able to convincingly turn such socio-economic information into a Tier 3 indicator of climate change impacts it will be highly policy relevant. There are, however, major challenges with this approach. Socio-economic observations generally integrate a large number of processes and climate change is only one of them. The issue itself may also be politically contentious. The case of human migration illustrates the difficulties very well. The impact of climate change on human migration is an important question, but can also lead to populist claims (Bettini and Andersson 2014, Brzoska and Fröhlich 2015). Careful statistical analysis may nevertheless provide important insights (Mueller, Gray, and Kosec 2014). This

[11] http://climate.copernicus.eu/

suggest that progress in determining Tier 3 climate change indicators using impact functions could be advanced by showing illustrative examples and making data available for explorative work through the Copernicus services. At the same time caveats should be stressed.

6. References

Arent, D.J., R.S.J. Tol, E. Faust, J.P. Hella, S. Kumar, K.M. Strzepek, F.L. Tóth, and D. Yan, (2014) Key economic sectors and services. In: Climate Change 2014: Impacts, Adaptation, and Vulnerability. Part A: Global and Sectoral Aspects. Contribution of Working Group II to the Fifth Assessment Report of the Intergovernmental Panel on Climate Change Cambridge University Press, Cambridge, United Kingdom and New York, NY, USA, pp. 659-708.

Baccini, Michela, Annibale Biggeri, Gabriele Accetta, Tom Kosatsky, Klea Katsouyanni, Antonis Analitis, H. Ross Anderson (2008) Heat effects on mortality in 15 European cities, Epidemiology 19, no. 5: 711-719.

Ballester, J., Robine, J. M., Herrmann, F. R., & Rodó, X. (2011). Long-term projections and acclimatization scenarios of temperature-related mortality in Europe. Nature communications, 2, 358.

Bauler, Tom (2012) An Analytical Framework to Discuss the Usability of (environmental) Indicators for Policy, Ecological Indicators, Indicators of environmental sustainability: From concept to applications, 17 (June): 38–45. doi:10.1016/j.ecolind.2011.05.013.

Bettini, Giovanni, and Elina Andersson (2014) Sand Waves and Human Tides: Exploring Environmental Myths on Desertification and Climate-Induced Migration, the Journal of Environment & Development 23 (1): 160–85. doi:10.1177/1070496513519896.

Boettle, M., J. P. Kropp, L. Reiber, O. Roithmeier, D. Rybski, and C. Walther (2011), About the influence of elevation model quality and small-scale damage functions on flood damage estimation, Nat. Hazards Earth Syst. Sci., 11 (12), 3327-3334, doi: 10.5194/nhess-11-3327-2011

Boyd E, Levitan M, van Heerden I (2005) Further specification of the dose-response relationship for flood fatality estimation. Paper presented at the US-Bangladesh workshop on innovation in windstorm/storm surge mitigation construction. National Science Foundation and Ministry of Disaster & Relief, Government of Bangladesh. Dhaka, 19–21 December 2005

Brzoska, Michael, and Christiane Fröhlich (2015) Climate Change, Migration and Violent Conflict: Vulnerabilities, Pathways and Adaptation Strategies, Migration and Development 0 (0): 1–21. doi:10.1080/21632324.2015.1022973.

Carvalho, A., M. D. Flannigan, K. Logan, Ana Isabel Miranda, and Carlos Borrego (2008). "Fire activity in Portugal and its relationship to weather and the Canadian Fire Weather Index System." *International Journal of Wildland Fire* 17, no. 3: 328-338.

Church, J. A., P. Clark, A. Cazenave, J. Gregory, S. Jevrejeva, A. Levermann, M. Merrifield, G. Milne, R.S.Nerem, P. Nunn, A. Payne, W. Pfeffer, D. Stammer, and A. Unnikrishnan (2013), Sea level change, in Climate Change 2013: The Physical Science Basis, edited by T. F. Stocker, D. Qin, G.-K. Plattner, M. Tignor, S. Allen, J. Boschung, A. Nauels, Y. Xia, V. Bex, and P. Midgley, Cambridge University Press, Cambridge, UK and New York, NY. USA.

CIESIN (2000) Columbia University. International Food Policy Research Institute (IFPRI) World Resources Institute (WRI) Gridded Population of the World (GPW) Version 2. CIESIN, Columbia University; Palisades, New York: 2000. Available at: http://sedac.ciesin.columbia.edu/plue/gpw.

Ciscar, J. C., Iglesias, A., Feyen, L., Szabó, L., Van Regemorter, D., Amelung, B., Soria, A. (2011). Physical and economic consequences of climate change in Europe. Proceedings of the National Academy of Sciences, 108(7), 2678-2683.

Cramer, W., G.W. Yohe, M. Auffhammer, C. Huggel, U. Molau, M.A.F. da Silva Dias, A. Solow, D.A. Stone, and L. Tibig (2014): Detection and attribution of observed impacts. In: Climate Change 2014: Impacts, Adaptation, and Vulnerability. Part A: Global and Sectoral Aspects. Contribution of Working Group II to the Fifth Assessment Report of the Intergovernmental Panel on Climate Change, Cambridge University Press, Cambridge, United Kingdom and New York, NY, USA, pp. 979-1037.

Delbart, N., Kergoat, L., Le Toan, T., L'Hermitte, J. and Picard, G. (2005) Determination of phenological dates in boreal regions using normalized difference water index. - Remote Sensing of Environment 97: 26-38.

Dilling, Lisa, and Maria Carmen Lemos (2011) Creating Usable Science: Opportunities and Constraints for Climate Knowledge Use and Their Implications for Science Policy, global Environmental Change, Special Issue on The Politics and Policy of Carbon Capture and Storage, 21 (2): 680–89. doi:10.1016/j.gloenvcha.2010.11.006.

DG Enterprise and Industry (2013) DEM over Europe from the GMES RDA project (EU-DEM, resolution 25m) - version 1.

Dunn, M.r., J.a. Lindesay, and M. Howden (2015) Spatial and Temporal Scales of Future Climate Information for Climate Change Adaptation in Viticulture: A Case Study of User Needs in the Australian Winegrape Sector, Australian Journal of Grape and Wine Research 21 (2): 226–39. doi:10.1111/ajgw.12138.

Dutta, Dushmanta, Srikantha Herath, and Katumi Musiake (2003), A mathematical model for flood loss estimation, *Journal of hydrology* 277, no. 1: 24-49.

EEA (2006). The thematic accuracy of CORINE land cover 2000. assessment using LUCAS (land use/cover area frame statistical survey). Technical Report no7/2006, European Environment Agency.

EEA (2012). Climate change, impacts and vulnerability in Europe 2012 an indicator-based report.

European Topic Centre on Land Use and Spatial Information (2013). Land-cover Corine datasets (1990, 2000 and 2006).

Füssel, H-M. (2010) Modeling impacts and adaptation in global IAMs. Wiley Interdisciplinary Reviews: Climate Change. DOI: 10.1002/wcc.40

Hajat, Shakoor, and Tom Kosatky (2010) Heat-related mortality: a review and exploration of heterogeneity, Journal of Epidemiology and Community Health 64, no. 9: 753-760.

Hinkel, Jochen, Robert J. Nicholls, Athanasios T. Vafeidis, Richard SJ Tol, and Thaleia Avagianou (2010) Assessing risk of and adaptation to sea-level rise in the European Union: an application of DIVA, Mitigation and Adaptation Strategies for Global Change 15: 703-719.

Hinkel, Jochen, Daniel Lincke, Athanasios T. Vafeidis, Mahé Perrette, Robert James Nicholls, Richard SJ Tol, Ben Marzeion, Xavier Fettweis, Cezar Ionescu, and Anders Levermann (2014), Coastal flood damage and adaptation costs under 21st century sea-level rise. *Proceedings of the National Academy of Sciences* 111, no. 9:: 3292-3297.

Huizinga, H. J. (2007) Flood damage functions for EU member states. Implemented in the framework of the contract #382442-F1SC awarded by the European Commission - Joint Research Centre.

IWGSCC (2010) Technical Update of the Social Cost of Carbon for Regulatory Impact Analysis Under Executive Order 12866. Technical Support Document. Interagency Working Group on Social Cost of Carbon, United States Government

Lobell, David B., Wolfram Schlenker, and Justin Costa-Roberts (2011) Climate trends and global crop production since 1980, Science 333, no. 6042: 616-620.

Mastrandrea, M. D. (2010) Representation of Climate Impacts in Integrated Assessment Models. In Assessing the Benefits of Avoided Climate Change: Cost Benefit Analysis and Beyond. Gulledge, J., L. J. Richardson, L. Adkins, and S. Seidel (eds.), Proceedings of Workshop on Assessing the Benefits of Avoided Climate Change, March 16–17, 2009. Pew Center on Global Climate Change: Arlington, VA, p. 85–99. Available at: http://www.pewclimate.org/events/2009/benefitsworkshop

Mendelsohn, Robert, Ariel Dinar, and Apurva Sanghi. (2001), The effect of development on the climate sensitivity of agriculture" *Environment and Development Economics* 6, no. 01: 85-101.

Merz, B., Kreibich, H., Schwarze, R., & Thieken, A. (2010). Review article: Assessment of economic flood damage, Natural Hazards and Earth System Science, 10(8), 1697-1724.

Metsämäki S., Kristin Böttcher, Matias Takala, Jouni Pulliainen, Kari Luojus, Juval Cohen (2015) Detection of snow melt-off using opticAl and microwave Earth observation snow data – a study for Europe. Author S.. Oral presentation given at IGARSS-conference. (Unpublished)

Mueller, V., C. Gray, and K. Kosec (2014) Heat Stress Increases Long-Term Human Migration in Rural Pakistan, Nature Climate Change 4 (3): 182–85. doi:10.1038/nclimate2103.

Nordhaus, W. D. (1992). An Optimal Transition Path for Controlling Greenhouse Gases. Science, 258: 1315 –1319. DOI 10.1126/science.258.5086.1315

Ortiz, R.A. and A. Markandya (2009) Integrated Impact Assessment Models of Climate Change with an Emphasis on Damage Functions: a Literature Review. Basque Centre for Climate Change (BC3)

Osborne, Tom M., and Timothy R. Wheeler (2013) Evidence for a climate signal in trends of global crop yield variability over the past 50 years, Environmental Research Letters 8, no. 2:024001.

Patt, A.G., D. P. van Vuuren, F. Berkhout, A. Aaheim, A. F. Hof, M. Isaac and R. Mechler, (2010). Adaptation in integrated assessment modeling: where do we stand? Climatic Change 99:383–402. DOI 10.1007/s10584-009-9687-y

Pausas, Juli G. (2004), Changes in fire and climate in the eastern Iberian Peninsula (Mediterranean basin)." *Climatic change* 63, no. 3: 337-350.

Pausas, Juli G., and Susana Paula. "Fuel shapes the fire–climate relationship: evidence from Mediterranean ecosystems." *Global Ecology and Biogeography* 21, no. 11 (2012): 1074-1082.

Pindyck, R.S. (2013). Climate Change Policy: What do the models tell us? Working Paper 19244. National Bureau of Economic Research, Cambridge, USA

Pinheiro, J., Bates, D., DebRoy, S., Sarkar, D. and R Core Team (2014). Nlme: Linear and Nonlinear Mixed Effects Models. R package version 3.1-118.

Poulter, B., and Patrick N. Halpin (2009) Raster modelling of coastal flooding from sea-level rise, International Journal of Geographical Information Science 22, no. 2: 167-182.

Prahl, B. F., D. Rybski, J. P. Kropp, O. Burghoff, and H. Held (2012), Applying stochastic small-scale damage functions to German winter storms, Geophys. Res. Lett., 39, L06806, doi:10.1029/2012GL050961

Preethi, B., and J. V. Revadekar. (2013), Kharif foodgrain yield and daily summer monsoon precipitation over India. *International Journal of Climatology* 33, no. 8: 1978-1986.

Revadekar, J. V., and B. Preethi (2012), Statistical analysis of the relationship between summer monsoon precipitation extremes and foodgrain yield over India, *International Journal of Climatology* 32, no. 3: 419-429.

R Core Team (2014). R: A language and environment for statistical computing. - R Foundation for Statistical Computing.
Schlenker, W., & Roberts, M. J. (2009). Nonlinear temperature effects indicate severe damages to US crop yields under climate change. Proceedings of the National Academy of sciences, 106(37), 15594-15598.

Steadman R (1984) A Universal Scale of Apparent Temperature. Journal of Climate and Applied Meteorology 23:1674:1687

Stern, Nicholas (2007). The Economics of Climate Change: The Stern Review. Cambridge University Press

Tribbia, John, and Susanne C. Moser. (2008). “More than Information: What Coastal Managers Need to Plan for Climate Change.” Environmental Science & Policy 11 (4): 315–28. doi:10.1016/j.envsci.2008.01.003.

Vafeidis, A. T., R. J. Nicholls, L. McFadden, R. S. J. Tol, J. Hinkel, T. Spencer, P. S. Grashoff, G. Boot, and R. J. T. Klein (2008). A new global coastal database for impact and vulnerability analysis to sea-level rise. In: Journal of Coastal Research 24.4, pp. 917–924. doi: 10.2112/06-0725.1.

Van den Hengel D (2006) Slachtoffers bij overstromingen: analyse van een slachtoffermodel aan de hand van de Watersnoodramp van 1953 en overstromingssimulaties. MSc thesis, Delft University

Valtonen, A., Leinonen, R., Pöyry, J., Roininen, H., Tuomela, J. and Ayres, M. P. (2014). Is climate warming more consequential towards poles? The phenology of Lepidoptera in Finland. - Global Change Biology 20: 16-27.

Venäläinen, A., Tuomenvirta, H., Pirinen, P. and Drebs, A. (2005) A basic Finnish climate data set 1961–2000—description and illustrations. Finnish Meteorological Institute, Reports 5:1–27

Vermeer, Martin, and Stefan Rahmstorf (2009). "Global sea level linked to global temperature." Proceedings of the National Academy of Sciences 106, no. 51: 21527-21532.

Vickery, P. J., Skerlj, P. F., Lin, J., Twisdale Jr, L. A., Young, M. A., & Lavelle, F. M. (2006). HAZUS-MH hurricane model methodology. II: Damage and loss estimation. Natural Hazards Review, 7(2), 94-103

Warren, Rachel, C. Hope, M. Mastrandrea, R. S. J. Tol, W. N. Adger, and Lorenzoni, (2006). Spotlighting the impacts functions in integrated assessments. Research Report Prepared for the Stern Review on the Economics of Climate Change. Tyndall Centre Working Paper 91

Weitzman, M. L. (2010). What is the "damages function" for global warming – and what difference might it make? Climate Change Economics, 01(01): 57. DOI 10.1142/S2010007810000042.